

Hospital Surge Capacity for an Influenza Pandemic in the Triangle Region of North Carolina

Rachel Woodul

Honors Thesis

Supervised by: Dr. Paul Delamater

Reader: Dr. Mike Emch

Department of Geography, The University of North Carolina at Chapel Hill

Approved by: _____

Advisor: Dr. Paul Delamater

Approved by: _____

Reader: Dr. Mike Emch

Introduction

Influenza, or flu, is a contagious respiratory illness caused by infection of the nose, throat, and lungs by an influenza virus. Infection can cause mild to severe illness, with serious cases requiring hospitalization and potentially resulting in death (“Influenza (Flu) Viruses | Seasonal Influenza (Flu) | CDC,” 2017). Influenza is highly contagious; it is spread through droplets emitted when an infected person coughs, sneezes, or talks, and can be spread to others from a distance of up to six feet (“How Flu Spreads | Seasonal Influenza (Flu) | CDC,” 2017). Symptoms of influenza infection typically develop 1-4 days after exposure, and infected individuals are able to spread the virus to others beginning at ~1 day before the onset of symptoms and ~5-7 days after becoming ill (“How Flu Spreads | Seasonal Influenza (Flu) | CDC,” 2017). Because of the highly infectious nature of the virus and the natural susceptibility of the human population (without vaccination), the United States often experiences a seasonal influenza pandemic. A seasonal influenza epidemic is typically caused by a virus that is a slightly mutated version of the virus from the previous year’s seasonal epidemic (“Types of Influenza Viruses | Seasonal Influenza (Flu) | CDC,” 2017), resulting in a level of residual immunity in the population. Residual immunity occurs when an individual has been exposed to and developed an immune response to a virus and this prior exposure is similar enough to a new virus to offer some level of immune protection, although the protection is often lessened (Medina et al., 2010; Pérez-Trallero, Piñeiro, Vicente, Montes, & Cilla, 2009).

Influenza viruses circulate year-round, however, most of the cases of influenza in the United States occur between December and February (“Seasonal Influenza, More Information | Seasonal Influenza (Flu) | CDC,” 2017). In most patients, seasonal influenza can be treated with antiviral drugs, which lessen symptoms and shorten the time an individual feels ill by several

days (“Treatment | Seasonal Influenza (Flu) | CDC,” n.d.). Serious cases of influenza may require hospitalization and usage of a ventilator, and may potentially be fatal. The U.S. Centers for Disease Control and Prevention (CDC) estimates that seasonal influenza in the United States results in between 9.2 million and 35.6 million illnesses, between 140,000 and 710,000 hospitalizations, and between 12,000 and 56,000 deaths annually (“Disease Burden of Influenza | Seasonal Influenza (Flu) | CDC,” 2017). The actual impact rates of seasonal influenza vary greatly from year to year based on the strain of influenza virus that has become epidemic during that season.

Sometimes, though, a different type of influenza virus emerges; a virus that is both a result of natural genetic variation and unlike any other circulating strain. In these cases, the strain is entirely novel, in that there is no vaccine available to combat diffusion and it is so dissimilar from any previously circulating strain that there is no residual immunity in the human population. This unique variation in viral strain is the greatest contributor to occurrences of pandemic influenza (Monto, Comanor, Shay, & Thompson, 2006). Given little existing immunity in the human population, the attack rate for this type of virus will be much higher than that of a typical influenza virus and many people will become ill. Because of the nature of infectivity of influenza, a majority of people will be able to transmit the virus before they realize they have been infected, and some individuals will spread the virus despite experiencing very few symptoms. Though rare, what may have started as a small outbreak or even a local epidemic of a novel influenza virus can quickly become a pandemic.

Some “high risk” demographic groups, including young children and the elderly, are the most likely to have serious complications from influenza infection. However, an entirely novel virus could change who is affected, how strongly they are affected, who needs medical care, the

type of care that is needed, and the volume of care that is required. When compared to a typical seasonal influenza epidemic, a novel influenza strain that becomes pandemic could increase death rates by more than 56% (“How Is Pandemic Flu Different from Seasonal Flu?,” 2017), quickly overwhelming health care systems and having catastrophic consequences.

There have been four influenza pandemics since 1900; taking place in 1918, 1957, 1968, and 2009. The 2009 H1N1 influenza A pandemic, known colloquially as “swine flu”, was first detected in the United States (“Past Pandemics | Pandemic Influenza (Flu) | CDC,” 2017) and is the most recent influenza pandemic at the time of this writing. However, the 1918 H1N1 influenza A pandemic, or the “Spanish Flu” pandemic, is probably the most well-known. About one-third of the world’s population became infected and more than 50 million people worldwide died as a result of infection (Morens & Fauci, 2007), making it the most severe influenza pandemic in recent years (“Past Pandemics | Pandemic Influenza (Flu) | CDC,” 2017) and one of the deadliest public health crises in human history (Morens & Fauci, 2007).

Should a pandemic with the same infectivity parameters as the 1918 Spanish Flu pandemic occur today, the number of both infected individuals and fatalities would greatly exceed typical rates of seasonal influenza. Because the population today is much larger, it is likely that both counts would also surpass those of all three pandemics of the twentieth century and potentially the 2009 H1N1 swine influenza pandemic. Though this seems like a doomsday scenario, it is not as hyperbolic as one would think. At the time of writing, the peak influenza-like-illness (ILI) activity level (or percent of overall visits to a healthcare facility attributed to influenza) for the 2017-2018 seasonal influenza epidemic was 7.7%. The peak ILI level for the 2009 H1N1 swine flu pandemic was 7.7% and the average ILI level for a seasonal epidemic is 2.2% (“Situation Update,” 2018). Such an elevated ILI for a seasonal epidemic is demonstrative

of the ways that population size can influence the size of an outbreak or pandemic, potentially contributing to the pandemic potential of the agent.

ILI levels are indicative of the magnitude of individuals that will demand care from healthcare facilities throughout the course of an epidemic or pandemic, and unusually high ILI levels may result in unexpected increase in demand for care. The ability of the healthcare system to respond to this increased demand for care is known as “surge capacity” (Barbisch & Koenig, 2006). Often, healthcare facilities will erect temporary facilities in parking lots and transform available space like hallways and waiting areas into patient care areas to meet this increased demand. During such a competition for hospital resources, it is likely that many individuals accessing or attempting to access hospitals may not be able to realize their access, or utilize health care services due to the still finite amount of resources available. Especially in large-scale crisis events, an individual’s ability to utilize resources may be limited by their physical distance from the health care facility. Distance decay, a governing law in spatial analysis, allows the assumption to be made that individuals located closer to the facilities will be able to physically access the facility before individuals located further from the facility, thus giving them a higher potential to utilize hospital resources (Morrill, Earickson, & Rees, 1970).

The aim of this research is to construct a model to evaluate the ability of the healthcare system to provide care in the event of an influenza pandemic. Using the Raleigh-Durham-Chapel Hill metropolitan statistical area, also known as the Triangle, as a case study, I investigate how a pandemic similar to that of the 1918 Spanish Flu pandemic would affect the population of the Triangle and the ability of the hospital system to respond. I seek to answer the following questions:

1. If an influenza pandemic similar to that of the 1918 Spanish Flu pandemic were to occur, how would the population of the Triangle region of North Carolina be affected?
2. At what point during an influenza pandemic would the hospital system of the Triangle exceed its capacity to provide care to infected individuals?
3. When considering the effect geographic distance can have on the ability of individuals to utilize hospital resources, how many individuals will be unable to receive care and where will they be located?

Statistical and spatial modeling is used to simulate an influenza pandemic in the Triangle, and a capacitated shortest distance allocation model is used to apportion the infected population of the Triangle to the nearest hospital with available treatment space until the capacity of the system is exceeded.

The intellectual merit of this project is in its contribution to both the existing literature and the constantly evolving discussions regarding large-scale disaster planning, health care system response, and pandemic preparedness, as it specifically investigates the spatial aspect of health care administration in the event of a sudden increase in demand for care. It will aid in the understanding of surge capacity in existing hospital systems and enhance the ability of the healthcare system to respond to unpredicted health crises that affect a disproportionately high number of individuals. The integration of existing capacity parameters for each hospital in the study area makes this model a valuable tool for disaster planning in the Triangle region, since it visualizes the expected response of the system based on current capacity values of hospitals in the Triangle and reveal potential weaknesses in the system response. However, the model allows for flexible capacity parameters, enabling scenario modeling and making it easily adaptable to

other hospital systems outside of the Triangle region. Additionally, this novel application of facility level data highlights vulnerable geographies within the study area; geographies in which residents may be unable or unlikely to receive care in the event of an influenza pandemic, epidemic, or other large-scale disaster.

There is an urgent need for models such as this one, as demonstrated by the 2017-2018 seasonal influenza epidemic in the United States, which is still ongoing at the time of writing. Though a seasonal epidemic, not a pandemic, hospitals across the United States are exceeding surge capacity and beginning to implement alternative care sites for influenza patients (Karlamanla, n.d.). This is demonstrative of the observed inability of the existing system to provide care for an increased number of patients associated with seasonally epidemic influenza, suggesting an inadequacy in preparedness for pandemic influenza.

This model is flexible in its application; it can be implemented in any region given the availability of similar input data. It can be integrated with existing preparedness and response plans to evaluate the efficacy of the system response. Additionally, this model enhances the understanding of surge capacity created by existing capacity models, such as FluSurge, by incorporating the location of patients and facilities into its modeled system operations. FluSurge and other existing capacity models consider the effect that limited supply may have on the ability of a healthcare system to provide care, which this model also does. However, this model's novelty is in the consideration of distance as the factor that might allow an individual to utilize the limited resources before somebody else.

Background

Influenza is a contagious respiratory illness caused by influenza viruses. There are four types of influenza viruses, classified by antigenic type. Influenza A and B viruses are known as Human Influenza and cause seasonal epidemics. Influenza C typically causes only a mild respiratory illness in hosts, and Influenza D is not known to infect humans. Influenza A viruses are further classified based on two proteins found on the outer surface of the viral envelope, hemagglutinin (H) and neuraminidase (N), and the genetic strain. Influenza B is not classified by surface proteins, but is classified by lineage and strain (“Types of Influenza Viruses | Seasonal Influenza (Flu) | CDC,” 2017). Historically, pandemic influenza has been caused by an outbreak of a novel strain of Influenza A. Novel strains of influenza typically arise from one of two mechanisms: gene reassortment between human influenza viruses and animal influenza viruses or genome adaptation (Morens & Fauci, 2007). This new virus must be able to infect a human population easily, be easily transmissible among humans in an efficient and sustained fashion, and the population must have little or no pre-existing immunity (“Pandemic Influenza | Pandemic Influenza (Flu) | CDC,” 2017). Pandemic influenza is rare; there have been only three influenza pandemics in the twentieth century and one in the twenty-first century (“How Is Pandemic Flu Different from Seasonal Flu?,” 2017).

Although rare, influenza pandemics have had serious impacts on human populations. The 1918 influenza pandemic, known as Spanish Flu, is among the most deadly events in human history (Medina et al., 2010; Morens & Fauci, 2007). An estimated 50-100 million people worldwide died during this pandemic. The 1918 Spanish Flu virus was a strain of subtype H1N1 virus, and was the base virus from which genetic reassortment of descendent strains produced the 1957 and 2009 pandemics (Medina et al., 2010; Morens & Fauci, 2007). In 1968, a new H3N2

influenza virus emerged to spark a pandemic, and has since become endemic in human populations. Despite four subsequent pandemics, the 1918 Spanish Flu pandemic is still used as the standard of pandemic influenza from which to create preparedness plans.

Brundage (2006) modeled the impacts of clinical case rates of the 1918, 1957, and 1968 pandemics in two referent United States populations as measured in the years 1917 and 2006. He found that when applying the attack rates of past pandemics to the 2006 population of the United States, the 1957 and 1968 pandemic attack rates resulted in greater numbers of clinical cases and fatalities than the attack rate of the 1918 pandemic. This is unexpected, given the 1918 pandemic was the deadliest in human history (Brundage, 2006), though it may be explained by an increase in overall population and changes in the demographic structure of the population. The 2006 population of the United States was nearly two times larger than the population in 1918, and it has increased since the publication of the Brundage study. If the case fatality rate of the 1918 Spanish influenza pandemic, 2.5%, were applied to the 2016 United States population, the death rate would exceed 8 million people; this is roughly equivalent to the entire population of Virginia (Brundage, 2006; U. S. C. Bureau, n.d.; Osterholm, 2005).

Though the 1918 Spanish Flu pandemic remains the foundation of pandemic preparedness planning, impacts of other pandemics and severe influenza epidemics have been incorporated into pandemic preparedness planning. The 1997 outbreak of H5N1 avian influenza A in humans in Hong Kong catalyzed an increase in pandemic preparedness planning (“National Pandemic Strategy | Pandemic Influenza (Flu) | CDC,” 2017), as evidence suggests that the 1918 Spanish Influenza virus emerged from an avian-adapted influenza virus to become easily transmissible in human populations (Tumpey et al., 2005). Although H5N1 avian influenza is not currently transmissible by humans (Chan, 2002), this was the first emergence of H5N1 avian

influenza A as a zoonotic disease capable of making the jump from animals to humans (Chan, 2002; Germann, Kadau, Longini, & Macken, 2006). H5N1 is now endemic in avian hosts globally (Chan, 2002; “H5 Viruses in the United States | Avian Influenza (Flu),” n.d.; U.S. Homeland Security Council, n.d.) and has been integrated into Pandemic Influenza Preparedness Plans alongside H1N1 swine influenza viruses typically thought to have the ability to circulate in human populations.

An integral piece of pandemic preparedness planning is in-hospital preparations. It is likely that a novel influenza pandemic would quickly overwhelm current hospital infrastructure (Daugherty, Carlson, & Perl, 2010; Osterholm, 2005). The 2009 H1N1 swine influenza A pandemic highlighted the necessity of preparedness in a health care setting. At least 50% of health care workers infected during the pandemic were infected in a health care setting (Daugherty et al., 2010). During the outbreak of severe acute respiratory syndrome (SARS) in 2003, a respiratory disease spread in a similar fashion to influenza, many health care workers simply did not report for work (Osterholm, 2005). Due to the mechanism of disease transmission and probable timeline for vaccine production, it is likely that health care workers will require medical care at a rate similar to, if not higher than, the general public (Daugherty et al., 2010; Osterholm, 2005; Uscher-Pines, Omer, Barnett, Burke, & Balicer, 2006). However, there is potential for communities to recruit and train volunteers to fill vacated health care work positions.

Where hospitals may ultimately fall short in pandemic preparedness planning is not in personnel, but in space. An influenza outbreak of any size, pandemic or not, has the potential to overwhelm licensed hospital bed space and the resources apportioned to each bed. Demand for ventilators, for example, would quickly exceed the number of ventilators available. Currently,

there are about 105,000 ventilators in the United States and between 75,000 and 85,000 are in use at any given time. A traditional seasonal flu requires over 100,000 ventilators, and a pandemic flu would potentially require two- or three- times as many (Osterholm, 2005). However, space would be the most valuable asset, as care cannot be delivered without proper space. A 2005 study of the potential impacts of pandemic influenza on critical services in England found that demand for hospital beds may exceed available hospital beds by more than 230% when not accounting for prevailing occupancy of beds by non-influenza patients (Menon, Taylor, Ridley, & on behalf of the Intensive Care Society, 2005).

The increased demand for physical space is known as “surge”, and the ability of a hospital to accommodate this sudden influx is known as “surge capacity” (Davis et al., 2005). Definitions of surge capacity vary greatly throughout the literature, thus producing a single, coherent definition is difficult. Hick, Barbera, and Kelen (2009) propose a framework with which to refine the definition of surge capacity by identifying levels of available space, staff, and supplies. The first level of surge capacity, Conventional Capacity, is the space, staff, and supplies consistent with daily operations. Contingency, the second level of surge capacity, is a level of space, supplies, and staff not consistent with daily operations but having minimal impact on patient care. Crisis capacity, the third level, involves the implementation of adaptive spaces and potential shortages of staff and supplies with the goal of providing sufficient patient care (Hick, Barbera, & Kelen, 2009). This framework builds upon the work of Barbisch and Koenig (2006), which sought to identify the essential components of an effective health care system response to surge. Four essential components of an effective response were identified: staff, staff, space, and system/structure (Barbisch & Koenig, 2006; Watson, Rudge, & Coker, 2013). These components originate in the definition of surge capacity published by the Joint

Commission on Accreditation of Healthcare Organization, which states: “surge capacity encompasses potential patient beds; available space in which patients may be triaged, managed, vaccinated, decontaminated, or simply located; available personnel of all types; necessary medications; supplies and equipment; and even the legal capacity to deliver health care under situations which exceed authorized capacity” (Barbisch & Koenig, 2006). Of the four essential components, “space” is often emphasized as the most important component of an effective surge response (Hick et al., 2009; Joshi, 2008; Schultz & Stratton, 2007; Schultz & Koenig, 2006), with hospitals serving as the health care “system” or “structures” in which the space is operationalized.

It is important to conceptualize surge capacity of a hospital or healthcare system within the context of physical space, as lack of physical space often serves as a reliable proxy measure for lack of staff or equipment with which to respond to the needs of the sudden influx of patients. For the purposes of this paper, I will use the framework for defining surge capacity proposed by Hick, Barbera, and Kelen (2009). It is assumed that the hospitals within the study area are operating at Crisis Capacity, in order to attempt to accurately model the effects of a sudden influx of patients suffering from pandemic influenza on physical hospital space (and, by proxy, staff and resources). Thus, this study will be specifically examining the “space” and “system” components of an effective response to surge (Barbisch & Koenig, 2006; Watson et al., 2013).

Surge capacity is an essential part of pandemic preparedness. Currently, the United States Center for Disease Control and Prevention publishes and maintains a pandemic influenza simulation model, FluSurge 2.0, which quantifies the potential impacts of a pandemic in the context of expected hospital surge. FluSurge 2.0 is specifically designed to assess potential surge at a facility level and provide estimates of resource usage in the event of an influenza pandemic.

To provide an accurate result, FluSurge requires counts of beds and ventilators, count of infected individuals, length and virulence of the pandemic virus, and duration of hospital stay. Impacts of surge are reported as potential hospital visits and hospital stays, beds used, the percentage of admissions that will require a bed in an Intensive Care Unit (ICU), and potential ventilators needed (“FluSurge 2.0 | Pandemic Influenza (Flu) | CDC,” n.d.). Although it provides a thorough output of estimated surge impacts, FluSurge can only be used to model surge at one facility, as opposed to a system of facilities that may work together. Additionally, FluSurge is reliant on user-input infectivity parameters. Because of this, there is the risk that the input pandemic parameters are not plausible in the population served by the modeled facility and thus, the output of modeled surge response may not be accurate. It is also important to note that FluSurge is a model of potential impacts in one user-generated scenario and should not be used as a tool to estimate accurately the impacts of a specific influenza pandemic. However, as a pandemic model, the integration of surge capacity and potential population case rates makes FluSurge a valuable tool to include in assessing pandemic preparedness of health care facilities. Menon, Taylor, and Ridley (2005) utilized a previous version of FluSurge (1.0) to create their assessment of potential impacts of an influenza pandemic in England. By modelling a surge in demand for hospital care based on an 8-week epidemic and a 25% attack rate, Menon et al. (2005) found that not only would demand exceed conventional capacity by more than 230%, but over 75% of ICU beds would be occupied by influenza patients at any given time during the epidemic. A shortcoming in the FluSurge 2.0 model and concepts of surge capacity, highlighted by Menon et al. (2005), is that FluSurge 2.0 provides estimates of surge and demand under the assumption that all hospital beds are vacant and able to be used in a surge response. Surge capacity, as a defined threshold at which a hospital could operate effectively to provide sufficient patient care

in the event of a sudden influx of patients, assumes all hospital beds and potential care spaces to be empty and able to be utilized. This, however, is not reflective of the reality of hospital operations. There would likely be long-term care patients or patients suffering from acute illnesses (non-influenza) filling hospital beds, and potential space for surge response may not be realistically operational were an influenza pandemic to begin without warning. It is likely that potential care spaces would require adaptation before they are able to be operationalized for patient care.

Theoretical Background

Spatial accessibility to health care is an important concept in both health care administration and in health geography and it is becoming an increasingly more relevant question in health crisis planning. Should there be a scenario in which large numbers of the population need care at the same time comprehensive knowledge regarding the ability of the healthcare system to administer care to large numbers of people will be crucial. However, the individuals must first be able to access the healthcare system. There have been many attempts to model the ability of the population to access the healthcare system; a few of the more popular models include simple supply-demand ratios, gravity models, and floating catchment area metrics. This research utilizes a capacitated allocation model to simulate access. The allocation method draws on the theoretical bases of container metrics, gravity models, and floating catchment areas to inform its own method of considering access, and the method of modeling utilization of facilities by infected individuals originates in the theoretical bases of Huff Models.

Container-based metrics

Container-based metrics, also known as supply-demand ratios, are among the simplest measures of spatial accessibility. A ‘container’, often a pre-existing boundary, is applied to the study area and individuals that are located within the container are assumed to utilize the healthcare facility within the study area. The count of services available at the facility is the supply, and the number of the individuals within the container become the demand, generating a measure of services available per individual. However, this metric fails to consider the theoretical nature of boundaries. If the container boundary is a county line, for example, individuals who may be located on the border of two counties may not seek care at the facility assigned to their container, but may instead access a facility in the adjoining county because it is physically closer to them. Additionally, this metric is reliant on the size and location of the container to generate its measure of accessibility. The ratio of services per individual at one facility will vary drastically between a container large enough to capture 1000 people and a container only large enough to capture 10 people. The location of the container boundaries also directly influence the metric, as boundaries can be moved to include or exclude individuals from the service area of the facility, altering the resulting ratio.

Gravity Models

Hansen (1959) developed a gravity model to investigate potential spatial accessibility, originally intended to examine the ways in which access to employment shapes land use around metropolitan areas. In the Hansen model, access is defined as the potential for opportunities for interaction (Hansen, 1959). Access, then, is a generalization of the relationship between the population of an area and the distance they must travel to take advantage of the opportunity being studied. This model operationalizes access as a measure of the spatial distribution of the

opportunities, and this distribution is adjusted for the geographic separation of the population and the opportunities, written as:

$${}_1A_2 = \frac{S_2}{T_{1-2}^x}$$

where

{}_1A_2 is a relative measure of the accessibility at point 1 to the opportunity at point 2

*S*₂ is the size of the opportunity at point 2

*T*₁₋₂ is the travel time or distance between point 1 and point 2

x is an exponent describing the effect of the travel time or distance between point 1 and point 2

(Hansen, 1959)

Access (*A*) at point 1 to the opportunity at point 2 is directly proportional to the size (*S*) of the opportunity and is inversely proportional to some function of the distance (*x*) separating point 1 from point 2. The total accessibility experienced by individuals located at point 1 is defined by the summation of the accessibility measures to each of the opportunities in the study. The function of distance (*x*) is an attempt to capture the notion that an individual's willingness to traverse a distance is dependent upon the purpose of the travel. Hansen proposed exponents of 2.20 for work-related travel, 2.35 for social travel, and 3.00 for shopping-related travel. The function of distance does not include a function of distance for healthcare-related travel, thus making the original gravity-based model less than optimal for visualizing population access to healthcare services.

Joseph and Bantock (1982) were among the first researchers to apply measures of potential accessibility to health geography, and adapted a gravity model to do so. They determined that given a maximum range per service offered and assuming that each individual in the study population is a potential user of the service, the spatial pattern of physical accessibility

to the service will be dependent upon the relative location of the population and the service. Using access to general practitioners as a case-study with which to model potential access to services, they proposed the following gravity model:

$$A_i = \sum_j G P_j / d_{ij}^b.$$

where

A_i is potential physical access of the population of area i to general practitioners

GP_j is the general practitioner at point j within the range of area i

d_{ij} is the distance between i and j

b is a function of distance

(Joseph & Bantock, 1982)

To capture the effect that population demand, a function of population size, may have on the availability of services, Joseph and Bantock (1982) proposed a subsequent model for estimating differential availability of services, represented as differential availability of physicians:

$$D_j = \sum_i P_i / d_{ij}^b$$

Where the demand on a physician (D_j) at point j is a function of the population size within the service area of point j (or within the maximum range per service offered) modified by the distance from the population to point j . Joseph and Bantock (1982) then combine these equations to create an adapted gravity model that captures the effect that differential availability of service will have on potential access to healthcare (A_i^*). In the case study, services are again represented by access to general practitioners (GP).

$$A_i^* = \sum_j [GP_j / \sum_i P_i / d_{ij}^b] / d_{ij}^b.$$

Because this model focuses on the relationship between the physical distance separating the population and the service while also considering the effect of the demand the population exerts on the service, only data on population distribution and service location is needed (Joseph & Bantock, 1982). It is a simple, yet useful measure of the potential geographic accessibility of populations to healthcare services.

Floating Catchment Areas

Floating catchment area (FCA) metrics are based on gravity models, and incorporate service supply, potential population demand and differential availability, and physical distance into their estimation of spatial accessibility to healthcare services (Delamater, 2013). There are many versions of floating catchment area models, with several of the metrics improving upon the previous one. Though FCA metrics are gravity-based models, a notable difference between FCA metrics and gravity models is that FCA metrics attempt to merge measurements of spatial accessibility and differential availability into a single measurement representative of the overall accessibility of services by the population (Delamater, 2013; Guagliardo, 2004). This measurement of accessibility is assigned to the geographic area as X amount of service (i.e. physicians, hospital beds, etc.) per Y amount of the population, demonstrating the services available to the population considering the physical accessibility of the population to each service and the magnitude of available services within the catchment area.

Huff Model

The Huff Model (Huff, 1963, 1964) is designed to capture the probability (P) that an individual (i) will utilize a facility (j) when presented with the option of multiple facilities, given that the utility of j is relative to the sum of the utility of all other facilities (n) considered by the individual (i):

$$P_{ij} = U_j / \sum_{j=1}^n U_j$$

In this model, choice behavior is viewed as probabilistic and is dependent upon the perceived utility of the facility. The perceived utility is any variable or parameter upon which the individual is assumed by the model to give preference to one facility over another. To adapt this model to capture the probability of choosing healthcare facilities, utility (U) is changed to capacity (C), which may be represented by the service being studied (i.e. physicians, hospitals beds, etc.) (J. Luo, 2014). By doing this, the utility of the facility to the individual, the factor by which they are assumed to make their decision, is actually the capacity of the facility to provide care.

Additionally, distance (d_{ij}) and a distance impedance coefficient ($-\beta$) is incorporated into the model to consider the effects that travel time may have on an individual's choice behavior (J. Luo, 2014). The Huff Model for quantifying probability of utilization of a healthcare service site can then be written as:

$$P_{ij} = C_j d_{ij}^{-\beta} / \sum_{j=1}^n C_j d_{ij}^{-\beta}$$

Capacitated shortest-distance allocation model

The allocation model presented in this paper adapts accessibility metrics to simulate population access in order to measure utilization. Joseph and Bantock's (1982) adapted gravity model will serve as the basis for the component of capacity in the model acting as a limiting feature of facilities. Though capacity is typically considered an attracting factor (Joseph & Bantock, 1982; J. Luo, 2014), it will be considered the limiting factor in the ability of individuals to utilize health care. By doing so, the model will measure not the ability of the population to access a facility as a floating catchment area metric would, but their ability to realize access through facility utilization. However, the effect of service supply on access is being investigated in a similar fashion to floating catchment area metrics. Instead of assigning a measurement of access to specific population points, as a floating catchment area would, this model considers the level of access at specific population points. Unlike a floating catchment area metric, this model outputs the ability of the population to access and utilize facilities, rather than potential access of the population. Although not a container-based metric, the model will utilize a type of container in simulating access to facilities. Specifically, the boundaries of the study area serve as the container, so to limit the population to accessing only facilities within the study area. The allocation method by which individuals are assigned to access their nearest facility comes from the Huff Model (Huff; 1963, 1964) of probabilistic selection behavior, in that the utility variable is distance from the individual. A closer facility will have a higher perceived utility value and thus a higher probability of utilization.

Methods and Materials

Study Area

The Raleigh-Durham-Chapel Hill Metropolitan Statistical Area of North Carolina, also known as the Triangle region or, more colloquially, “the Triangle”, is the second largest metropolitan region in North Carolina (U. S. C. Bureau, n.d.). The region is made up of seven counties, which vary from highly urbanized to rural. Anchored by The University of North Carolina at Chapel Hill, Duke University, and North Carolina State University, the Triangle also contains fourteen other universities and colleges, as well as the Research Triangle Park, the largest research park in the world (“About The RTP,” n.d.), from which it takes its name. When studying access to and utilization of health care, the Triangle presents an interesting case study. The population is highly mobile and is demographically diverse. Because of the abundance of educational institutions and the Research Triangle Park, there are highly concentrated centers of young adults near the urbanized areas. Within the boundaries of the study area are eleven hospitals, two of which are major research hospitals. The health care infrastructure is well developed, however the socioeconomic status of the population is variable from place to place within the study area (U. C. Bureau, n.d.).

In the Triangle, there are both private and public health care facilities. The UNC Health Care system, based at the University of North Carolina at Chapel Hill, is the public health care complex of the state of North Carolina and offers primary and specialty care in addition to operating public hospitals and outpatient clinics throughout the seven county region. Duke Health, based at Duke University in Durham, is the other major hospital and outpatient clinic complex in the region; however, Duke Health is a private health care provider. Several hospitals in the region are operated under a joint venture between Duke Health and LifePoint Health.

There is at least one hospital per county, with one exception; there is no hospital in Franklin County as of October 2015.

Location of Hospitals in the Triangle region of North Carolina

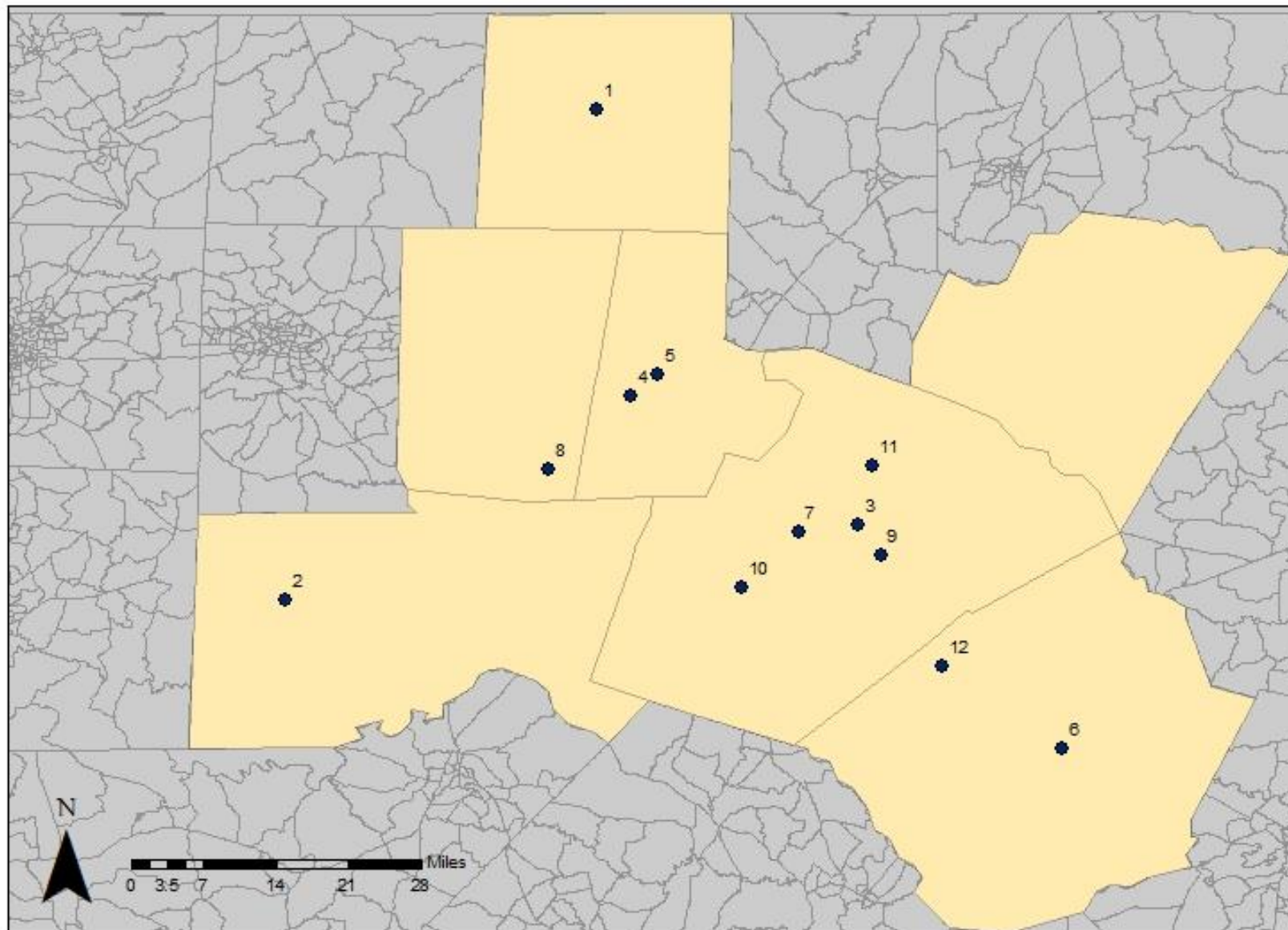


Figure 1 – Location of Hospitals in the Triangle

<u>Hospital ID</u>	<u>Capacity (beds)</u>
1	38
2	68
3	186
4	924
5	316
6	155
7	388
8	621
9	628
10	156
11	61
12	50

Table 1- Number of beds per hospital

Data acquisition and pre-processing

Shapefiles of census block groups for North Carolina and tables of the 2010 population by age group by sex for North Carolina were downloaded from the IPUMS National Historical Geographic Information System database, maintained by the Institute for Social Research and Data Innovation at the University of Minnesota (Manson et al., 2012). I combined population counts by age group by gender to create total population counts by age group for each census block group in North Carolina. I then joined the counts to the census block group shapefile and clipped the resulting shapefile to the size of the study area.

The spatial data file of hospital locations was downloaded from the NC OneMap GeoSpatial Portal, and attribute values of licensed bed numbers were referenced to a registry published and maintained by the North Carolina Department of Health and Human Services – Division of Health Service Regulation.

Location of Hospitals in the Triangle region of North Carolina

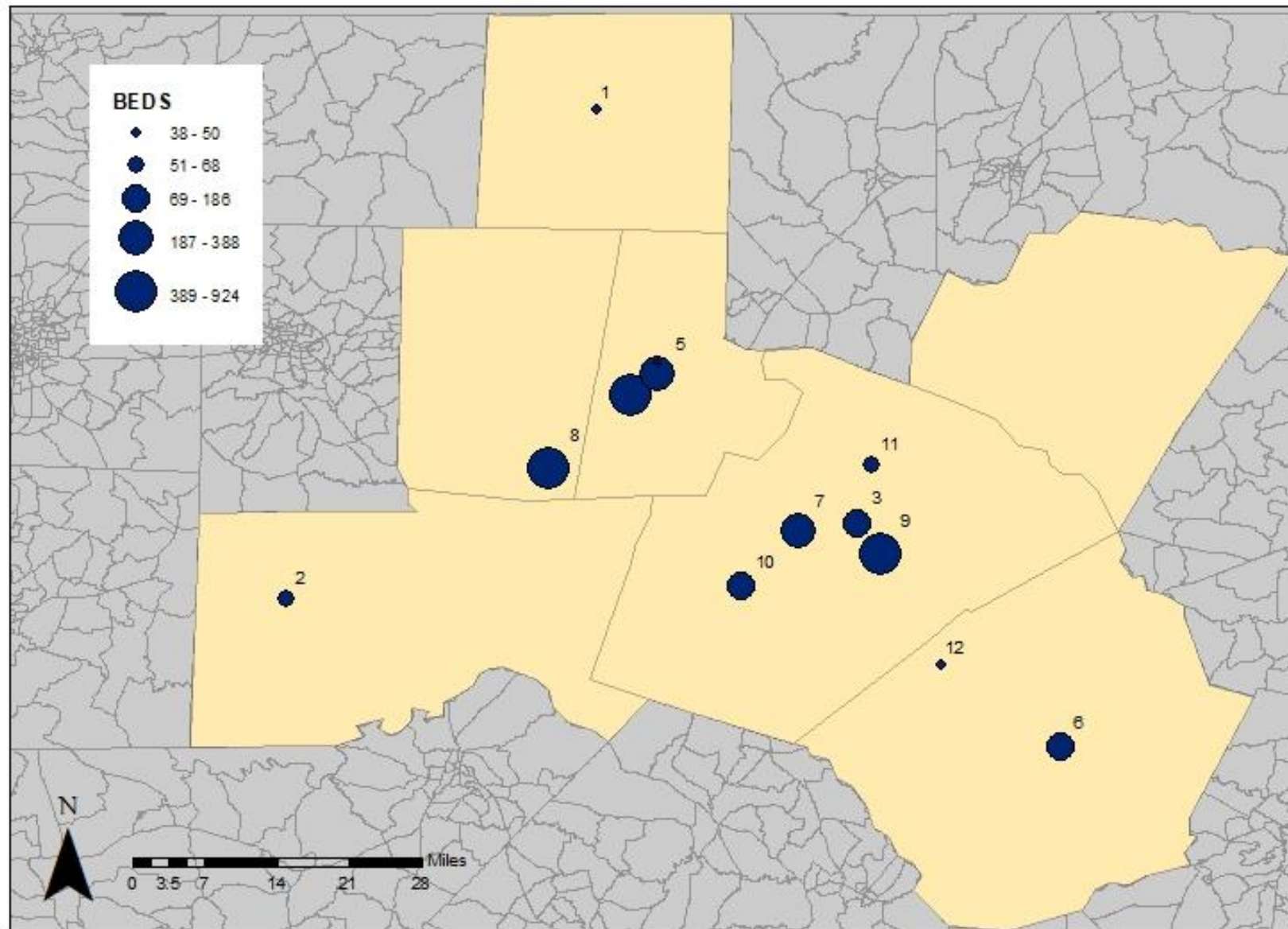


Figure 2 – Location and relative size of hospitals in the Triangle

The road network shapefile for North Carolina was downloaded from the North Carolina Department of Transportation. The roads shapefile required a significant amount of data cleaning in order to create a usable network dataset. First, connected road segments with similar attributes were dissolved. Road connectivity was enforced at intersections using planar topology. Digitizing errors (undershoots and overshoots) were fixed using ArcGIS' automated tools. After cleaning, the roads shapefile was converted to a road network layer.

I calculated geographic centroids for each census block group and located them on the road network. Hospital locations were also located on the network. Using this network, I conducted a shortest driving distance analysis from each census block group centroid to each hospital in the study area. This produced an origin-destination (OD) table with the block groups as the origins, the hospitals as the destinations, and the driving distance between each.

I estimated age group-specific clinical case rates from the 1918 Spanish Influenza using a graph published by the U.S. Army Center for Health Promotion and Preventive Medicine (Brundage, 2006) and the original 1919 mortality and case surveillance tables published by the U.S. Public Health Service (Frost, 1919, 1920; Frost & Sydenstricker, 1919). The age groups and clinical case rates are presented in Table 2.

To calculate the total number of expected flu cases in the Triangle region based on an outbreak similar to 1918, I multiplied the age group-specific clinical case rates by the corresponding age group population counts for census block group. This resulted in a count of total expected influenza cases per age group per census block group. The age group counts were summed for each block group and then summed over all block groups to create a count of total infected people for the study region by age group. The age group counts for the study area were then summed to calculate the total number of infected people for the entire study area. I also

calculated the relative proportion of infected people by age group for the study area by dividing the age group count by the study area count (Table 2).

Age group	CCR	POP	INF	INF(%)
0-4	32.0%	112,873	36,119	9.03%
5-9	37.5%	108,391	40,646	10.17%
10-14	36.0%	106,305	38,269	9.57%
15-19	33.0%	111,111	36,666	9.17%
20-24	32.0%	111,036	35,531	8.89%
25-29	32.5%	116,692	37,924	9.49%
30-34	32.0%	119,652	38,288	9.58%
35-39	28.0%	124,254	34,791	8.70%
40-44	22.5%	122,255	27,507	6.88%
45-49	20.0%	117,718	23,543	5.89%
50-54	16.0%	104,328	16,692	4.18%
55-59	13.0%	86,590	11,256	2.82%
60-64	12.0%	71,106	8,532	2.13%
65-69	11.5%	48,346	5,559	1.39%
70-74	10.0%	33,354	3,335	0.83%
≥ 75	8.0%	64,191	5,135	1.28%

Table 2 - Clinical case rates (CCR), populations (POP), estimated number of people infected (INF), and percent of all infected people (INF%) by age group.

SIR Model Development and Pandemic Simulation

A susceptible, infectious, and recovered (SIR) model without vital dynamics was used to simulate the daily counts of susceptible, infected, and recovered people in the study area, given similar characteristics to the 1918 Spanish Influenza and a modern population. An SIR model can be expressed by the following set of differential equations:

$$\frac{\Delta S}{\Delta t} = -\frac{\beta IS}{N},$$

$$\frac{\Delta I}{\Delta t} = \frac{\beta IS}{N} - \gamma I, \text{ and}$$

$$\frac{\Delta R}{\Delta t} = \gamma I$$

where S is the number of susceptible people at time t , I is the number of infected people at time t , R is the number of recovered people at time t , N is the total population count, β is the rate at which individuals move from susceptible to infected, and γ is the rate of recovery. The necessary input parameters to solve the SIR model were estimated using the age group-specific clinical case rates applied to the study area population (N).

Using the total count of infected persons, I estimated the infectivity parameters necessary to produce an influenza pandemic with the same clinical case rate as the 1918 Spanish Influenza in the 2010 population of the Triangle region. First, I divided the count of total infected persons for the study region by the total population of the study region (N) to create a proportion of the population infected by the end of the end of the pandemic event (z_f).

$$z_f = \frac{\text{count of total infected}}{N}$$

I then used the z_f value to estimate the R_0 value.

$$R_0 = -\frac{\log(1 - z_f)}{z_f}$$

I calculated the rate of recovery (γ) for the population using seven days as the average maximum infectious period in which an infected person is able to transmit the virus to a susceptible individual (“About Flu | Seasonal Influenza (Flu) | CDC,” 2017).

$$\gamma = \frac{1}{\textit{infectious period}}$$

Using the calculated rate of recovery (γ) and R_0 value, I then estimated the rate at which individuals will move from susceptible to infected (β) (Liu & Stechlinski, 2017).

$$\beta = R_0 * \gamma$$

Other parameters required to solve the SIR model were a pandemic time of 731 days, which is an estimation of the time of the 1918 Spanish Influenza (Barry, 2004), and a starting count of infected persons of 15 people (~.001% of the population). Setting the initial infected population at 15 people, rather than a single index case, was done to account for the potential that multiple infected individuals could enter the Triangle during a pandemic event due to the high mobility of the population. To solve the SIR model differential equations and simulate the pandemic, I used the deSolve library in R. The SIR model output for the total number of infected people in the Triangle region over the 731 day period was 399,583, which was nearly equal to the total number of infected people for the entire outbreak as estimated from the age group-specific clinical case rates (399,801).

The SIR model produced the total number of people infected for the entire study area per day, which needed to be redistributed back to the age groups and back to the block groups to produce the spatial distribution of infected people per day. The daily counts were first redistributed to age groups based on the relative percent values found in Table 2 by multiplying the daily count by the percent values for each group. The age group-specific daily counts were then redistributed back to the block groups based on the percent of the age group population in each block group. For example, the number of people aged 0-5 in block group 37013500107032 was 177 and the total number of people aged 0-5 in the study area was 112,873. As such block group 37013500107032 contained 0.15% of all people in this age group. If the age group-specific daily count of infected people was 74 (Day 285), block group 37013500107032 would have $74 * 0.15\% = .11$ infected people for this age group. This process was implemented for each block group and each age group to calculate the age group-specific counts of infected people per block group per day, which were then summed to calculate the total count of infected people per block group per day.

General Allocation Model Assumptions

For the purposes of this model, physical space with which to provide care was represented by number of hospital beds, which is used as a proxy for space, resources, and providers.

Because pandemic disease by its nature affects large numbers of the population in relatively similar ways, it can be assumed that affected members of the population within such a large geographic area will be attempting to access similar healthcare services. For the purpose of this study the infected population attempts only to access hospitals located within the boundaries of the study area. The model also assumes that all infected members of the population are

attempting to access healthcare facilities simultaneously each day; though this is not an entirely realistic scenario, it allows for the highly nuanced influence of distance on hospital utilization to be captured. Finally, the model assumes that individuals will attempt to access the facility closest to them with available space. This assumption is reliant on the Huff Model of probabilistic selection behavior, which states that individuals will choose the facility they perceive to have the highest utility value when utility is defined by considering distance and size (Huff, 1963, 1964; J. Luo, 2014). In this model, size is represented by capacity, not physical size.

Once an individual in this model has successfully utilized a facility, they will remain in the hospital, occupying a bed, for three days. (Davis et al., 2005) assessed surge capacity and discharge rates for mass-casualty events at multiple hospitals and found that, in a large portion of mass-casualty events, patients can be discharged within 24-72 hours after admission. In order to model the potential influence of length of stay on surge capacity for an influenza pandemic, I chose to model the hospitalization period as 72 hours.

Capacitated Shortest Distance Allocation to Hospitals

A capacitated shortest distance allocation model was developed for this study, wherein infected individuals in each census block group were allocated to their nearest hospital each day. In the model, allocated individuals that were hospitalized (utilized a bed) for three days (length of stay). The allocation model used an iterative process to assign infected individuals from each block group to the nearest hospital (for each day). To accomplish this, I first ordered the OD table of block group to hospital driving distances produced by the network analysis from shortest to longest distance. This was used this as the order in which infected individuals would attempt to access and utilize hospitals. The basic rules of the allocation model were as follows:

- If all infected people in a block group were allocated to the hospital, the remaining distance pairs (block group to hospital) for that block group were removed from the OD table.
- If the number of infected people in a block group was greater than the remaining capacity at the nearest hospital, the number that would bring the hospital to capacity were allocated to the hospital. The remaining number infected people for the block group was noted. Because the hospital's capacity was reached (could no longer accept people that day), the remaining distance pairs (block group to hospital) for that hospital were removed from the OD table.

For each day, the allocation of infected people continued by iterating through the distance OD table (which was updated after each iteration to account for the number of infected people allocated, the number of infected people remaining, and remaining hospital capacity) until all infected people were either hospitalized or hospital capacity was reached. If hospital capacity was exceeded, remaining individuals were considered to have been “turned away”, thus not receiving care. At the beginning of each successive day in the allocation model, for each hospital, the patients that had been hospitalized for three days were discharged (and removed from the hospital's capacity), while the patients that had been hospitalized for two days were shifted to being hospitalized for a third day and the patients that had been hospitalized the previous day were shifted to being hospitalized for a second day. As such, each hospital's remaining capacity was updated prior to the allocation process of each day's newly infected people. This allocation process was repeated for each day in the simulated pandemic.

Capacity Scenarios

In the first scenario of the infection and allocation model, maximum hospital capacity was set as the number of licensed beds for each hospital as reported by the North Carolina Department of Health and Human Services – Division of Health Service Regulation. This is reliant on the assumption that all licensed beds are available for in-patient care of individuals infected with influenza and that each licensed bed is accompanied by an appropriate supply of medications, ventilators, medical professionals, and other necessary supplies. Though somewhat unrealistic, this assumption was made to model a scenario in which all available hospital resources are directed towards treating pandemic influenza victims. This scenario allows for the assessment of the maximum licensed ability of the hospital system to provide care to pandemic influenza patients.

Two additional scenarios representative of both surge capacity operations and conventional capacity operations were created to investigate the effects of hospital capacity on the ability of the hospital system to provide care for the infected population.

The second iteration of the model represented maximum hospital capacity as double the number of licensed beds. This is representative of a scenario in which hospitals are able to provide one additional treatment space for each licensed bed. This scenario also assumes that all treatment spaces are available for in-patient care of individuals infected with influenza and that an appropriate supply of medications, ventilators, medical professionals, and other necessary supplies accompany each space. Provision of additional patient care spaces may include setting up alternate care sites in other public facilities, converting procedure suites into patient care spaces, providing temporary beds and cots in open spaces like hallways and lobbies, or erecting

temporary care clinics outside the hospital building in tents (Barbisch & Koenig, 2006; Davis et al., 2005; Eastman, Rinnert, Nemeth, Fowler, & Minei, 2007).

The third iteration of the model set maximum hospital capacity for people with influenza infections at 75% of the licensed beds. This scenario represents the likelihood that hospitals will have individuals already receiving in-patient care and utilizing beds and associated resources for general (non-influenza) acute care conditions. For the purposes of this model, all hospitals were assumed to begin with an initial occupancy of 25% of their licensed beds for providing general acute care.

Results

SIR Model and Pandemic Simulation

The following infectivity parameters were calculated, given the age group-specific clinical case rates, the age group-specific population of the study area, and the overall population of the study area: $z_f = .26$, $R_0 = 1.15$, $\gamma = .14$, and $\beta = 0.165$.

The results of the SIR model, given an outbreak period of 731 days and 15 initially infected individuals can be found for the S, I, and R compartments in Figures 3-5 and plotted together in Figure 6. The number of new infected individuals per day peaks at Day 368. Overall, 399,583 persons would become infected with influenza over the 731 day period. This is roughly a quarter of the population, as demonstrated by z_f .

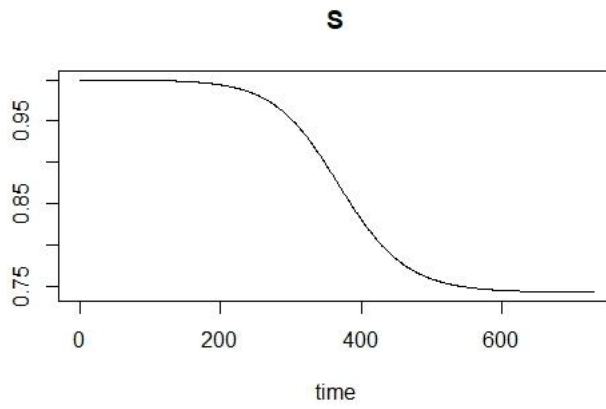


Figure 3 - Proportion of Population that is susceptible to influenza during the simulated pandemic

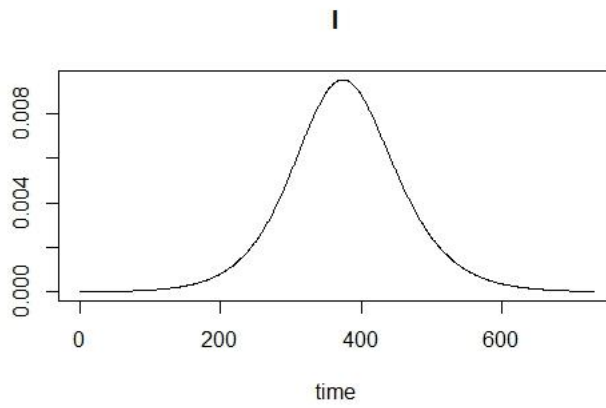


Figure 4 - Proportion of population that is infected with influenza during the pandemic

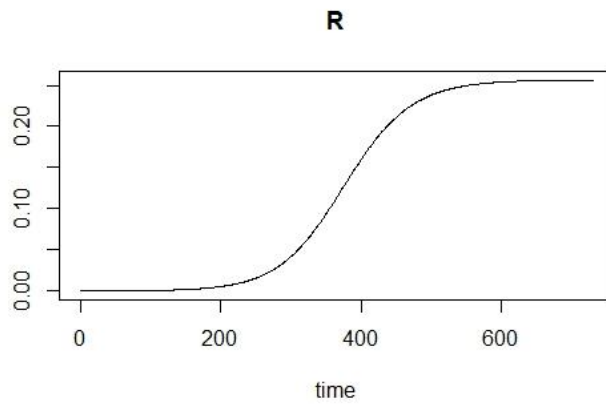


Figure 5 - Proportion of population that is recovered from influenza infection during the pandemic

SIR for a Simulated Influenza Pandemic

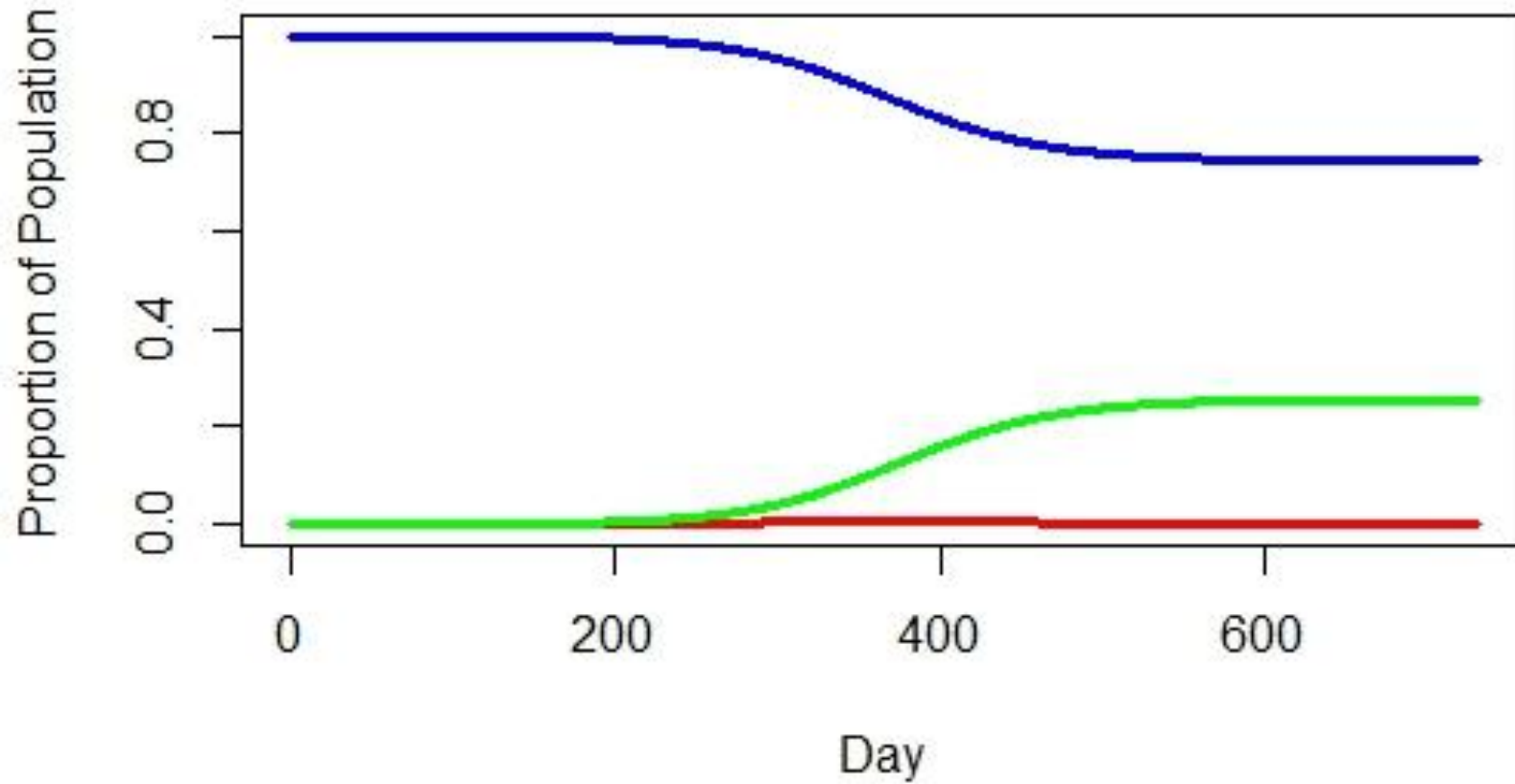


Figure 6- SIR Model

The output of the SIR model was a number of new infections per day, which was then allocated to age groups and block groups, to result in a total number of infected persons per block group for the entirety of the pandemic event (Figure 7). Based on the age distribution of the population at a block group level, this output is where infections are likely to take place in the Triangle as well as an estimate of number of infections per block group, should there be a pandemic. The variation in infection levels across the study area is likely due to the distribution of such a large population across the study area, however this model also accounts for the demographic age differences across the area.

Count of Infected Persons per Census Block Group

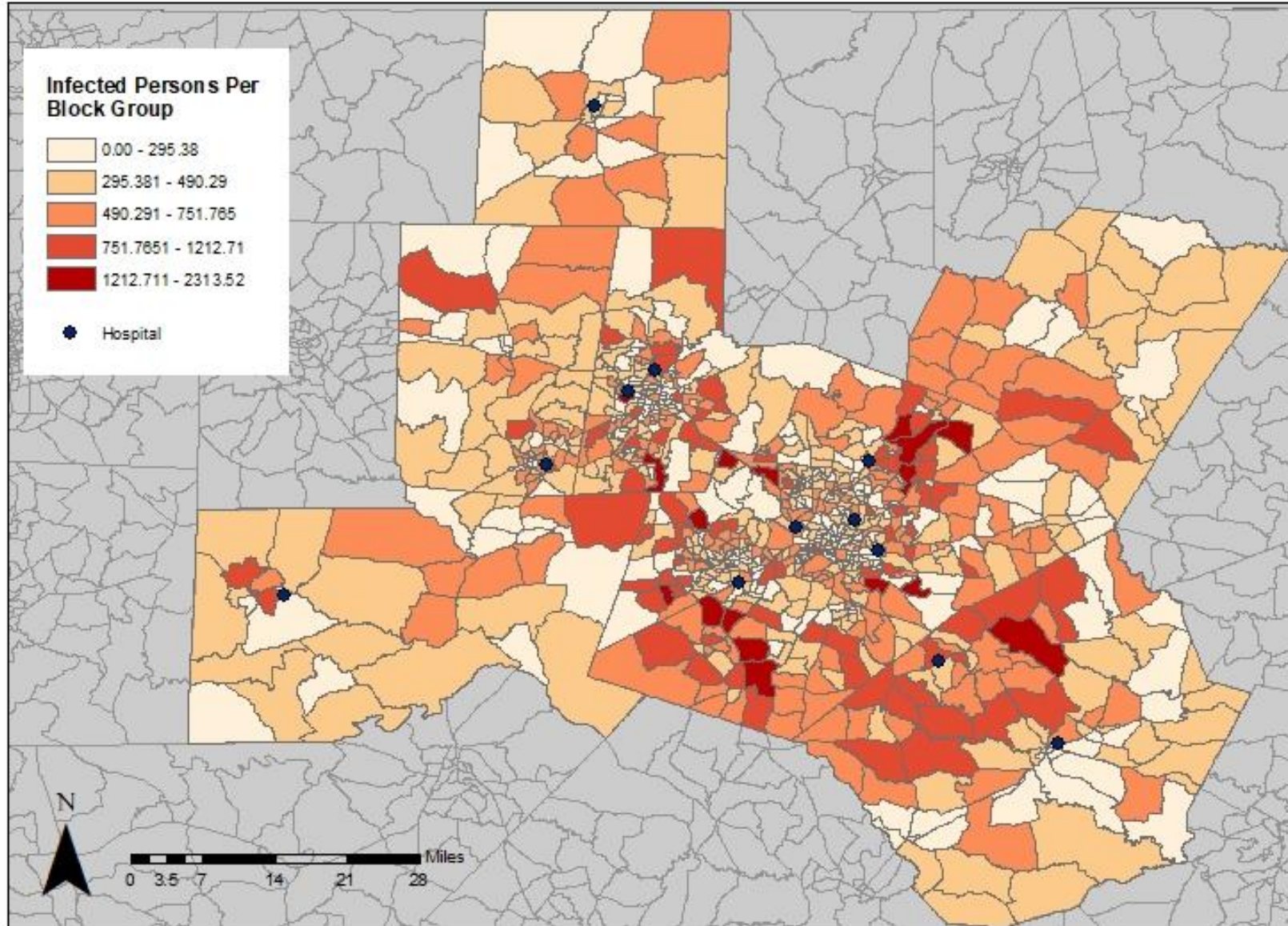


Figure 7 – Count of total infected persons per block group

Capacitated Shortest Distance Allocation Model

The first iteration of the capacitated shortest distance allocation model, which considered maximum hospital capacity to be the number of licensed beds as reported by the North Carolina Department of Health and Human Services – Division of Health Service Regulation, resulted in 317,141 individuals (79.4% of the infected population) being able to receive care. 82,485 individuals (20.6% of the infected population) would not be able to receive care. At its peak, demand for care exceeded available beds by ~126%. Capacity for each hospital in the study area was reached at various times throughout the study period (Table 3 and Figure 8). Capacity for all hospitals in the system is exceeded on Day 297 of the pandemic and maximum capacity is maintained until Day 445. Block groups located on the outer edges of the study area had higher rates of infected individuals being unable to utilize hospitals, however they did not necessarily have the highest counts of individuals unable to utilize hospital resources. Instead, the block groups immediately bordering the urban block groups of the study area had the highest counts of individuals unable to utilize hospital resources. This is likely due to the population distribution of the study area. Though the further block groups had higher percentages of the infected population unable to utilize hospitals, the populations of these block groups are smaller than the populations of the block groups located closer to urban centers. Though these block groups had a lower percentage of infected people unable to receive care, the size of their population resulted in a higher number of people unable to receive care (Figure 9, Figure 10).

Hospital ID	Capacity (beds)	Day Capacity is Reached
1	38	244
2	68	283
3	186	245
4	924	297
5	316	279
6	155	264
7	388	262
8	621	291
9	628	272
10	156	219
11	61	185
12	50	203

Table 3 - Day in pandemic event during which capacity is reached for each hospital in the study area

Occupancy per day for each Hospital in the Study Region

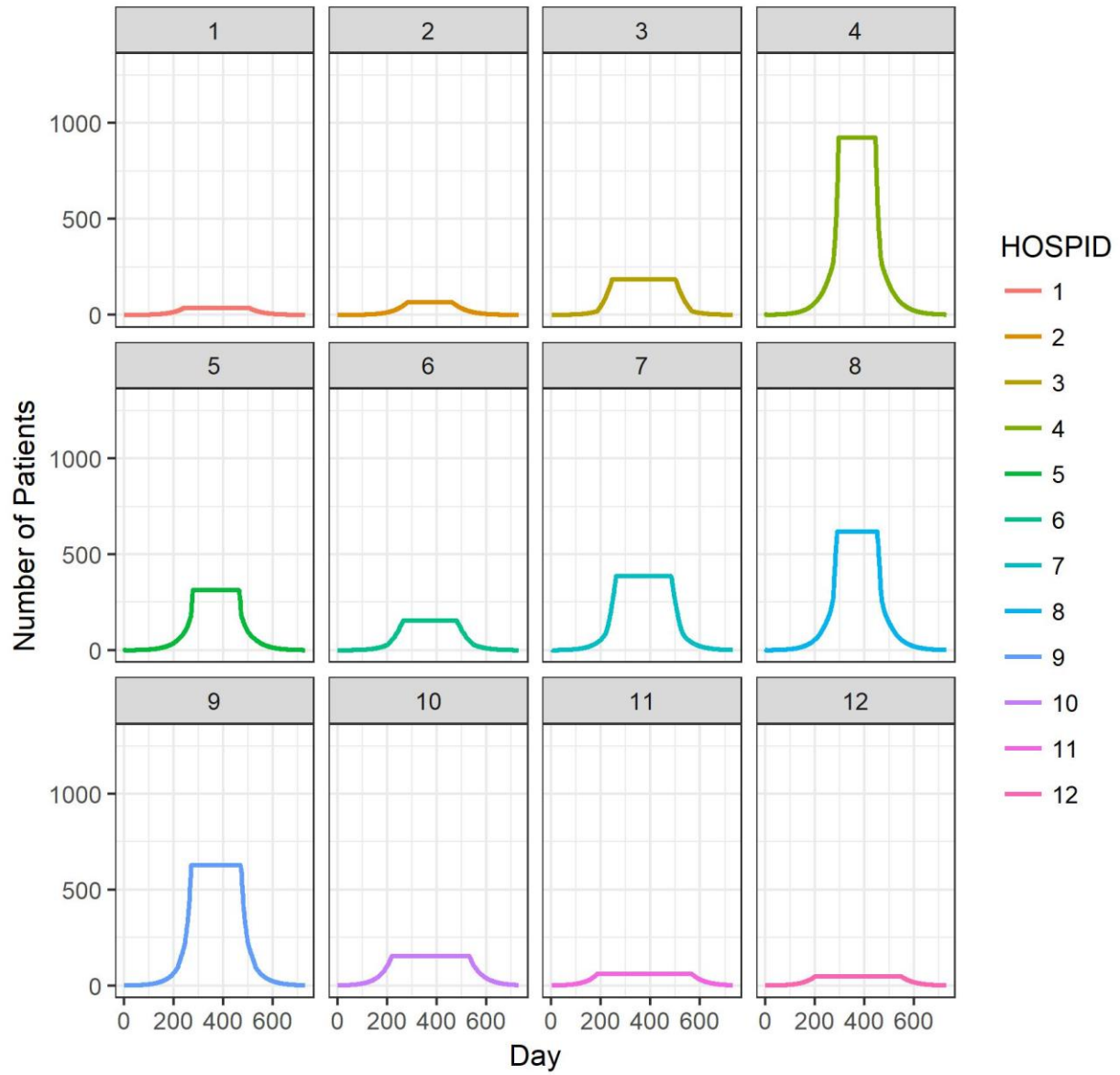


Figure 8 - Occupancy per hospital for the duration of the pandemic

Infected Individuals Unable to be Hospitalized

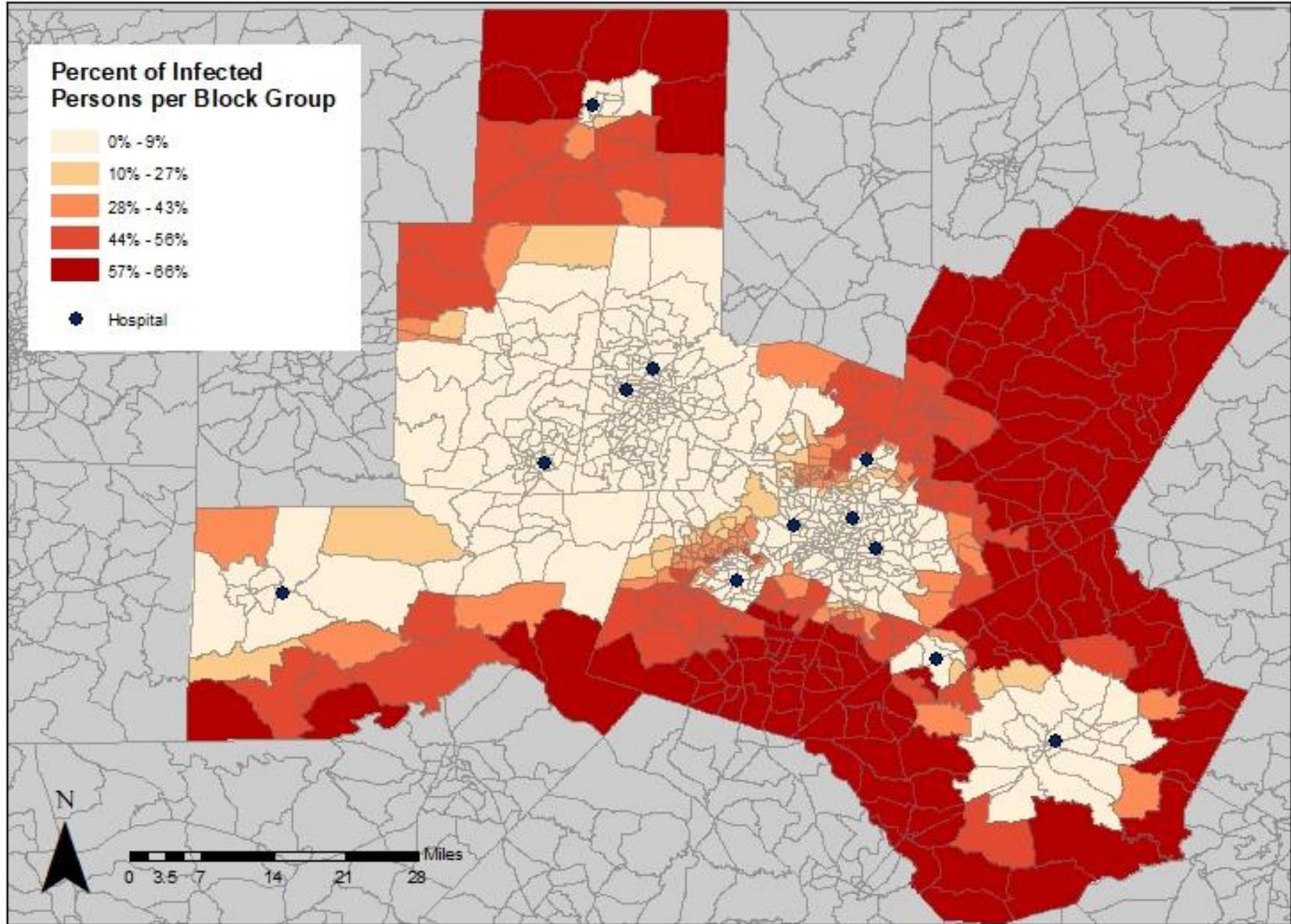


Figure 9 – Percent of Infected Population unable to receive care

Infected Individuals Unable to be Hospitalized

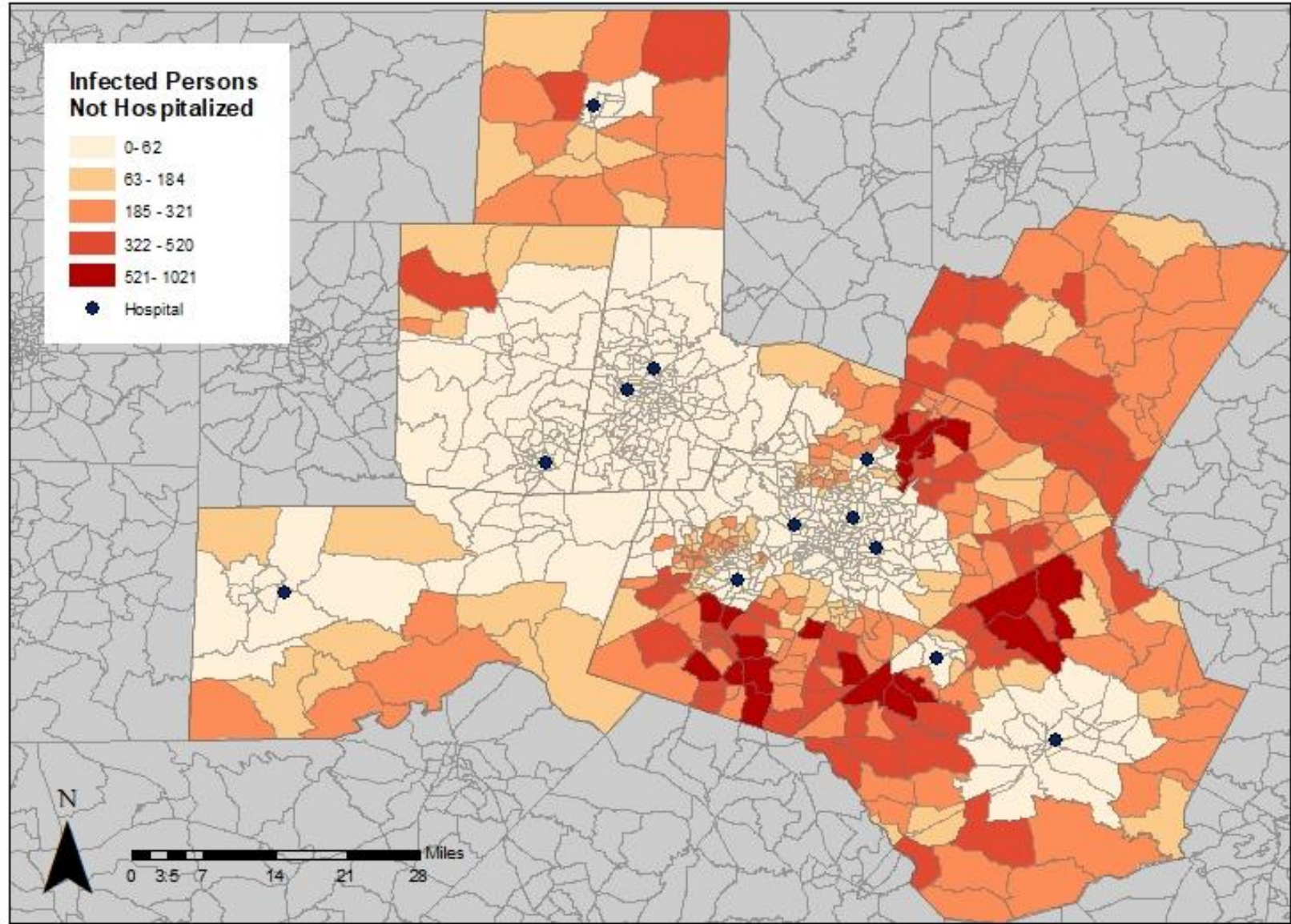


Figure 10 – Count of infected persons unable to receive care

The second iteration of the model, considering maximum hospital capacity to be double the number of licensed beds resulted in all infected individuals being able to receive care. Capacity for all hospitals in the system peaks at 87% on Day 380 of the pandemic (Table 4 and Figure 11). Notably, 10 of the 12 hospitals reached capacity, one hospital nearly reached capacity, and the largest hospital in the region was the only hospital with substantial capacity remaining.

Hospital ID	Capacity (beds)	Day Capacity is Reached	Peak Occupancy (Percent)
1	38	283	100%
2	68	344	100%
3	186	284	100%
4	924	370	60.90%
5	316	332	100%
6	155	308	100%
7	388	305	100%
8	621	370	93.70%
9	628	319	100%
10	156	253	100%
11	61	218	100%
12	50	237	100%

Table 4 – Day in pandemic at which occupancy peaks for each hospital in the study area, when each hospital is at 200% capacity

Occupancy per day for each Hospital in the Study Region

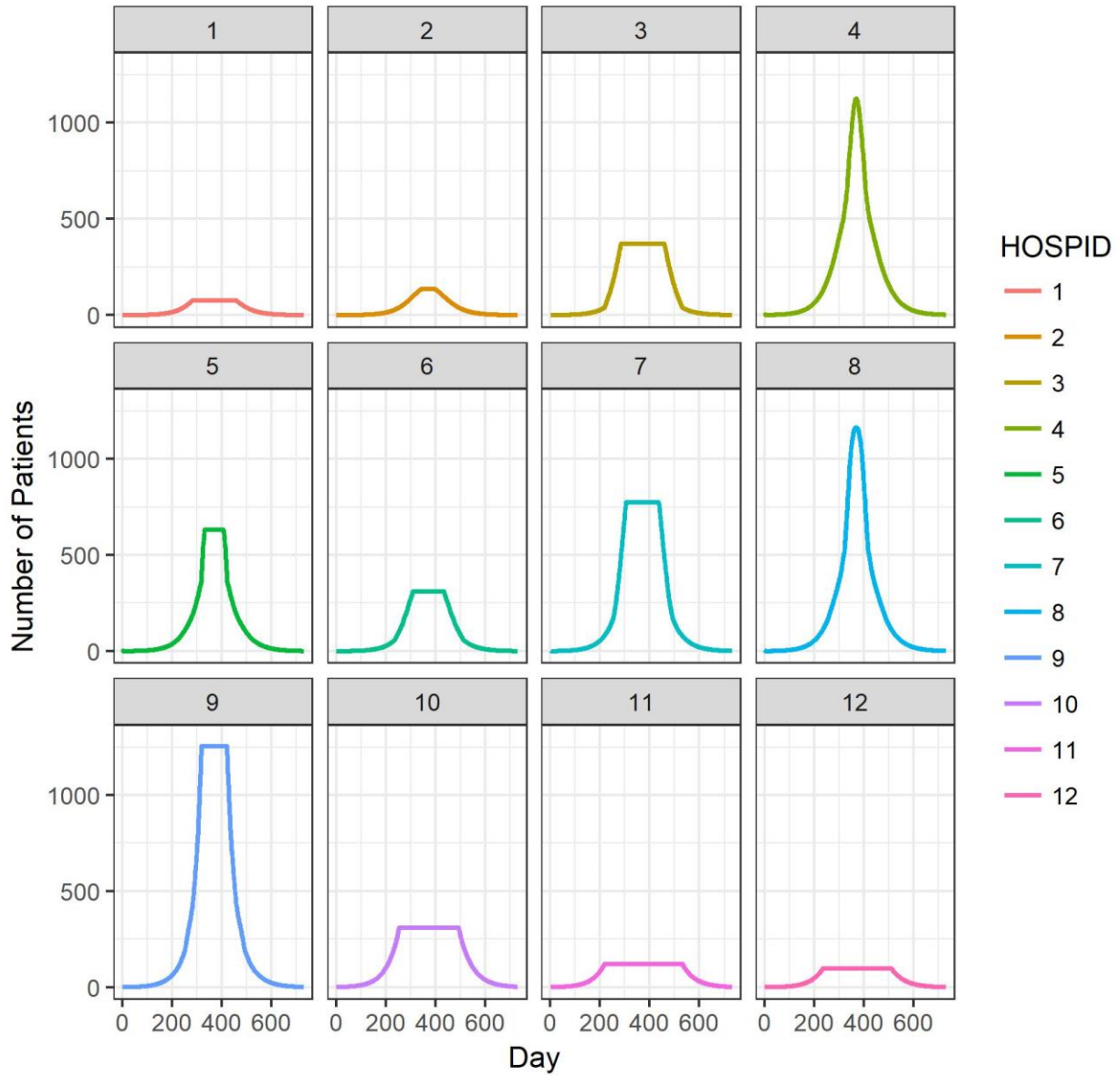


Figure 11 – Occupancy per day for each hospital in the study area, when each hospital is at 200% capacity

The third iteration of the model, in which maximum hospital capacity for people with influenza infections is set at 75% of the licensed beds resulted in 266,932 individuals (66.8% of the infected population) being able to receive care. 132,693 individuals (33.2% of the infected population) would not be able to receive care. At its peak, demand for care exceeded available beds by ~146%. Capacity for all hospitals in the system is exceeded on Day 278 of the pandemic, and occupancy remains at maximum capacity until Day 465 (Table 5 and Figure 12).

Hospital ID	Capacity (beds)	Day Capacity is Reached
1	38	230
2	68	267
3	186	231
4	924	278
5	316	262
6	155	249
7	388	246
8	621	274
9	628	256
10	156	205
11	61	172
12	50	189

Table 5 – Day during the pandemic during which capacity is exceeded for each hospital in the study area, when each hospital is at 75% capacity

Occupancy per day for each Hospital in the Study Region

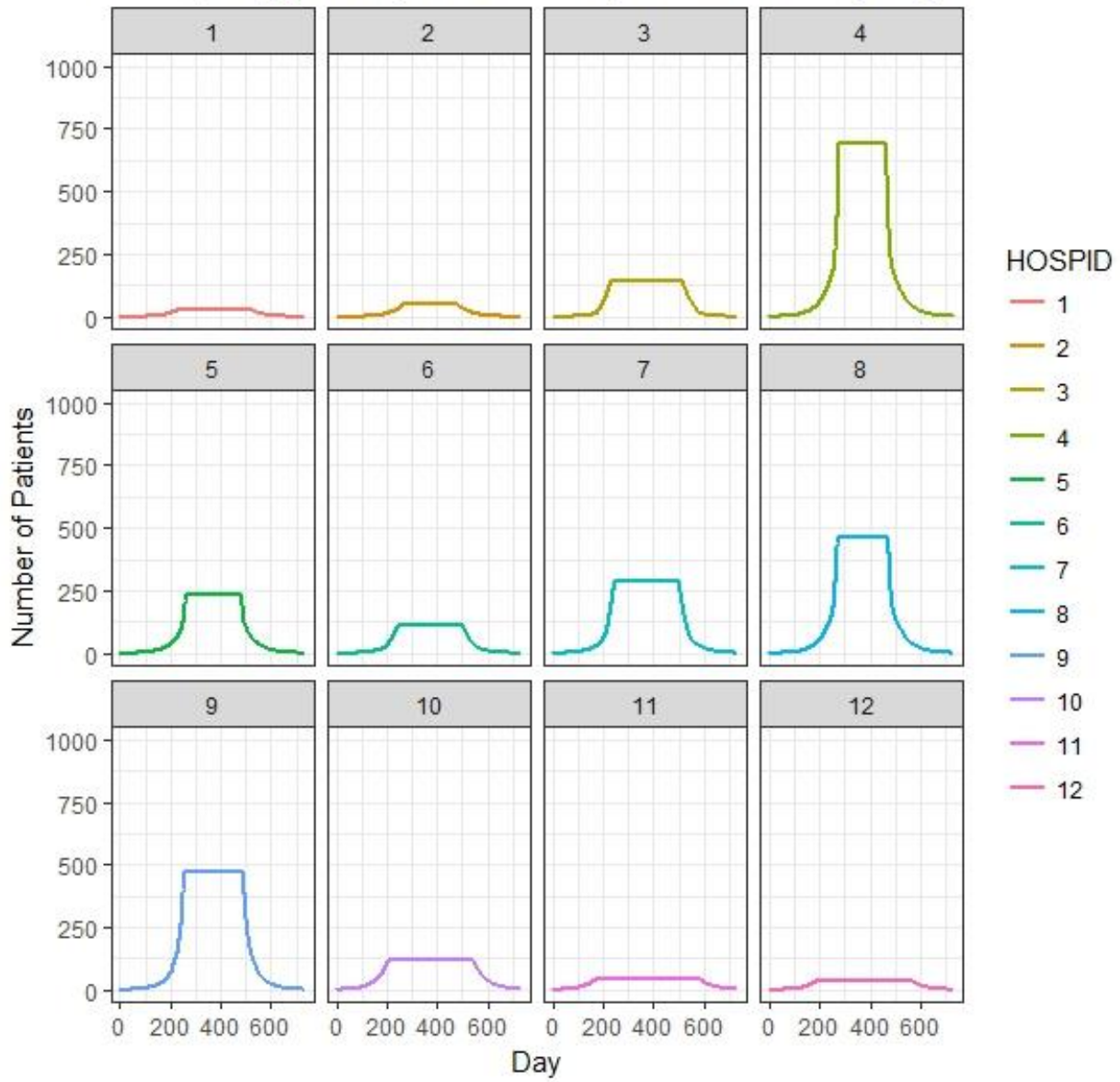


Figure 12 – Occupancy for each hospital in the study area per day, when each hospital is at 75% capacity

Discussion

Previous research has cited distance as an important variable in both access to health care services (Arcury et al., 2005; Joseph & Bantock, 1982; W. Luo & Wang, 2003) and utilization behavior (Arcury et al., 2005). However, previous research has also demonstrated a lack of association between geographic variables and acute health care visit behavior (Arcury et al., 2005; Gelberg, Andersen, & Leake, 2000), in that geographic distance may not influence an individual's decision to seek out acute care services. It is important to distinguish, though, that such research on access and utilization of health care services, whether for primary or acute care, has focused primarily on access and utilization behavior. In this study, access behavior was considered to be the same for all individuals in the study area, keeping with the findings of Gelberg, Andersen, & Leake (2000) that distance may not discourage an individual from seeking acute care services. All infected individuals in the simulated infected population were modeled to seek access to acute care services at their closest facility and all individuals were considered to have successfully accessed the facility to which they were allocated. However, a distinction was made in this study between access and utilization. All infected individuals were modeled to attempt to utilize hospital services, and their ability to successfully utilize services was dependent upon capacity of the facility to which they were allocated. In this way, the extent to which distance can exert a prohibitive effect on an individual's ability to utilize health care services when they are intent upon doing so could be investigated.

Additionally, this research has highlighted vulnerable geographies within the Triangle region in which distance from a hospital may prohibit a majority of the population from being able to receive care in the event of an influenza pandemic. In every block group in Franklin County at least 54% of infected individuals were unable to be hospitalized. There is no hospital

in Franklin County, thus the individuals located in these block groups had to overcome a greater distance to access a facility, making them less likely to be able to utilize services before an individual located closer to a facility (Figure 13).

Infected Individuals Unable to be Hospitalized

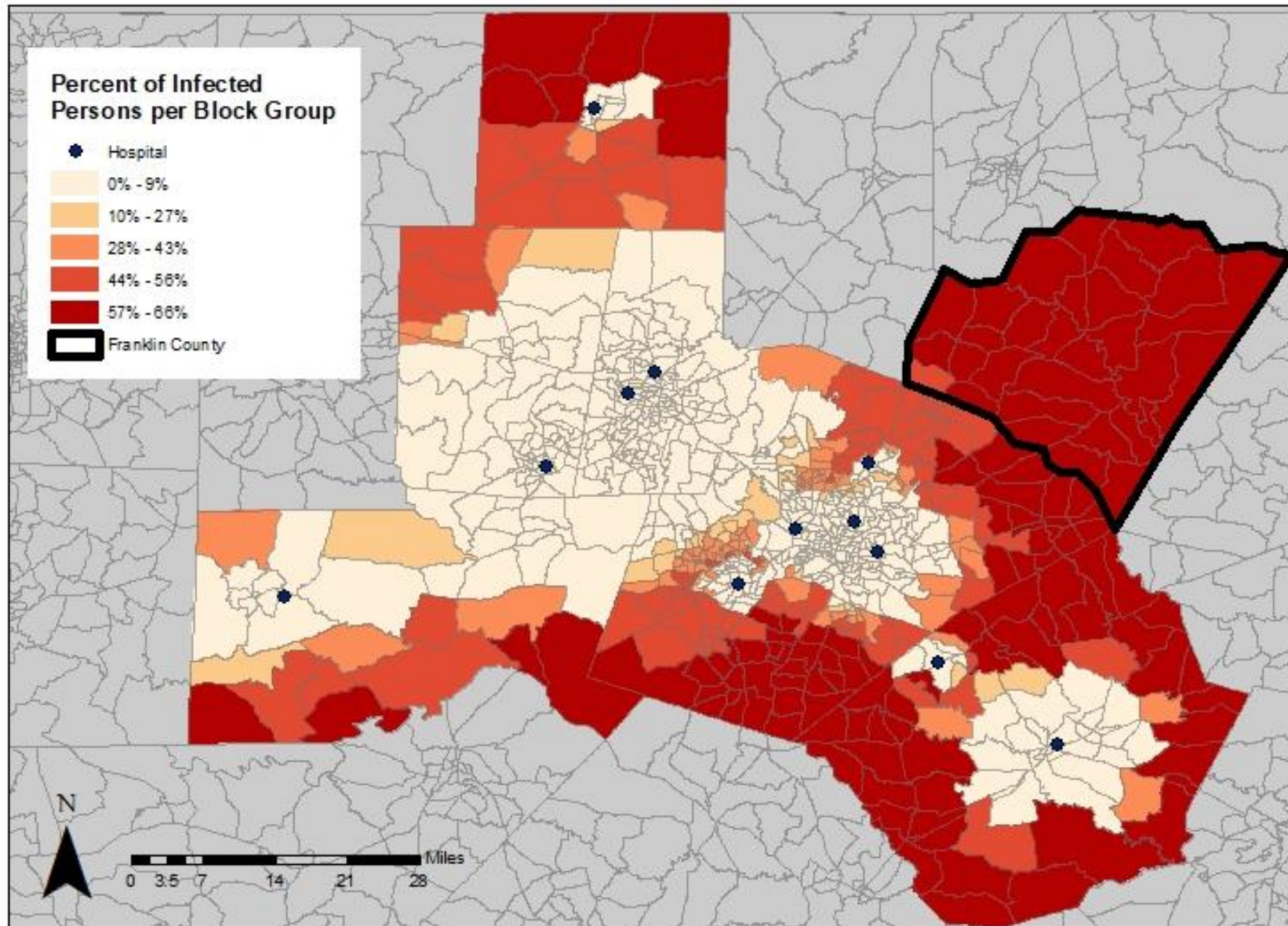


Figure 13 – Map of percent of infected individuals unable to be hospitalized per block group, with Franklin County highlighted

The percent of individuals unable to be hospitalized per block groups appears to decrease as distance from a facility increases, in somewhat of a radial pattern (Figure 9). Additionally, the hospitals with higher numbers of beds appear to have larger radii in which almost all infected individuals were able to get treatment (Table 1, Figure 2, Figure 10). The results of this case study suggest that geographic distance from facilities does have a prohibitive effect on the ability of an individual to utilize hospital resources, though the effect of distance could be mitigated by an increase in the capacity of the hospital system, as was demonstrated in the scenario in which hospital capacity was doubled. If all cases of individuals being unable to receive care are assumed to result in fatalities, the scenario with maximum capacity being the number of licensed beds per facility would result in a case fatality rate of ~2.0%. This is slightly lower than the case fatality rate of the 1918 Spanish Flu pandemic, which had a global case fatality rate of ~2.5%. The scenario in which maximum capacity was doubled resulted in no instances of individuals being unable to receive care, and thus no fatalities can be assumed for this scenario, making the case fatality rate 0.0%. However, a case fatality rate of 0.0% is extremely unlikely, as a typical seasonal influenza epidemic usually results in a case fatality rate of ~0.01% (“Disease Burden of Influenza | Seasonal Influenza (Flu) | CDC,” 2017; “How Is Pandemic Flu Different from Seasonal Flu?,” 2017; “Pandemic Influenza | Pandemic Influenza (Flu) | CDC,” 2017). The scenario in which maximum capacity was set at 75% of licensed beds to model the potential for there to be individuals already receiving in-patient care at the hospitals would result in a case fatality rate of ~33.2% if all individuals unable to be hospitalized were considered fatalities. Though these rates are dependent upon the assumption that lack of hospital care will result in a fatality, they are indicative of the importance of hospital capacity in preparing for and mitigating the deleterious effects of an influenza pandemic.

This research was not intended to be a predictor of magnitude or impact of future influenza pandemics, but rather to model the capacity of a specific health care system to provide care for the population in the event of an influenza pandemic. However, this model was reliant on several assumptions, and thus is subject to several limitations. The pandemic simulation did not consider the potential for vaccine development and distribution during a pandemic event, and also assumed absolutely no pre-existing immunity in the population, although other research has suggested that individuals who have lived through pandemic influenza events may have residual immunity against a following pandemic influenza event (Medina et al., 2010). Additionally, the model assumed that all infected individuals would attempt to utilize hospital resources, however, in an actual pandemic event there are possibilities for individuals to attempt to utilize health care facilities other than hospitals as well as not seek care at all. Further, this model did account for factors such as socioeconomic status, driver's license possession, car ownership, or other variables that may influence an individual's ability to seek care.

However, these limitations provide opportunities for future research in this field, specifically research that captures population-specific details such as vaccine availability and utilization, residual immunity, and health care access behavior. This understanding of hospital system capacity could potentially be integrated with existing location-allocation models to investigate where new facilities or temporary facilities could be located within a study area to most effectively provide care for the population in the event of a crisis or mass-casualty event. Additionally, this capacity model can be revised to model other crisis events in which an increased demand for care may be seen. Road and facility closures can be incorporated into this model to simulate potential system responses to crisis response barriers. This model is not

limited only to hospital capacity either; any facility in which capacity is a crucial element to operation can be input as the modeled facilities.

Conclusion

This study sought to understand how an influenza pandemic similar to that of the 1918 Spanish Flu pandemic would affect the population of the Triangle region of North Carolina, and the ability of the health care system to respond to the surging demand for care caused by such an event. By utilizing statistical and geospatial modeling to simulate an influenza pandemic, as well as through the creation of a capacitated shortest distance allocation model, this research has contributed to the discussions regarding large-scale disaster planning and pandemic preparedness by simulating a pandemic and visualizing the resulting ability of the population to utilize the hospital system.

The first question investigated in this research was: If an influenza pandemic similar to that of the 1918 Spanish Flu pandemic were to occur, how would the population of the Triangle region of North Carolina be affected? The results indicate that when considering only the ability to utilize health care facilities, a pandemic with an age-group specific clinical case rate the same as or similar to the 1918 Spanish Flu pandemic has the potential to result in a similarly high or higher case fatality rate in the population of the Triangle.

The second question posed by this study was: At what point during an influenza pandemic would the hospital system of the Triangle exceed its capacity to provide care to infected individuals? The first iteration of the model, in which maximum capacity for each hospital was equivalent to the number of licensed beds per hospital, resulted in system capacity

being exceeded on Day 445 of the pandemic event. The second iteration, in which maximum capacity was equivalent to double the number of licensed beds resulted in system capacity not being reached or exceeded. The third iteration of the model, in which maximum capacity was set at 75% of the licensed bed count, resulted in system capacity being exceeded on Day 278 of the pandemic event.

The third question that this study sought to answer was: When considering the effect geographic distance can have on the ability of individuals to utilize hospital resources, how many individuals will be unable to receive care and where will they be located? In the first iteration of the model, 82,485 individuals (20.6% of the infected population) were unable to receive care. A majority of the individuals unable to receive care were located in block groups along the outer edges of the study region, however every block group contained individuals unable to be hospitalized (Figure 10). The second iteration of the model resulted in all individuals being able to receive care. The third iteration of the model resulted in 132,693 individuals (33.2% of the infected population) unable to receive care.

The capacitated shortest distance allocation model developed during this research has the potential to be a valuable tool for furthering the discussions surrounding disaster planning, hospital system evaluation, and pandemic preparedness. Though this research focused specifically on the Triangle region of North Carolina, this model can be adapted for application to a variety of geographies.

Acknowledgements

Many thanks to Dr. Mike Emch in the UNC Department of Geography for serving as the reader for this thesis and to Dr. Ashley Ward for her support and editorial assistance during the completion of this thesis.

Thanks to Matt Jansen in the UNC Libraries Research Hub, Sarah Schmitt in the UNC Department of Geography, and Kelsey Sumner and Danielle Gartner at the UNC Gillings School of Global Public Health for their assistance and expertise in R.

Lastly, many thanks to Jordan Clark for reading and editing every draft of this paper, as well as to my roommate Miranda Veal for allowing me to constantly have the light on while she was sleeping so that I could complete this research.

Funding for this project was provided by the Tom and Elizabeth Long Research Award from Honors Carolina.

Works Cited

- About Flu | Seasonal Influenza (Flu) | CDC. (2017, October 5). Retrieved November 5, 2017, from <https://www.cdc.gov/flu/about/index.html>
- About The RTP. (n.d.). Retrieved April 15, 2018, from <https://www.rtp.org/about-us/>
- Arcury, T., Gesler Wilbert M., Preisser John S., Sherman Jill, Spencer John, & Perin Jamie. (2005). The Effects of Geography and Spatial Behavior on Health Care Utilization among the Residents of a Rural Region. *Health Services Research, 40*(1), 135–156. <https://doi.org/10.1111/j.1475-6773.2005.00346.x>
- Barbisch, D. F., & Koenig, K. L. (2006). Understanding Surge Capacity: Essential Elements. *Academic Emergency Medicine, 13*(11), 1098–1102. <https://doi.org/10.1197/j.aem.2006.06.041>
- Barry, J. (2004). *The Great Influenza: The Story of the Deadliest Pandemic in History*. New York: Penguin Group.
- Brundage, J. F. (2006). Cases and Deaths During Influenza Pandemics in the United States. *American Journal of Preventive Medicine, 31*(3), 252–256. <https://doi.org/10.1016/j.amepre.2006.04.005>
- Bureau, U. C. (n.d.). State Population Totals Tables: 2010-2016. Retrieved November 7, 2017, from <https://www.census.gov/data/tables/2016/demo/popest/state-total.html>
- Bureau, U. S. C. (n.d.). 2016 Population Estimates. Retrieved November 15, 2017, from https://factfinder.census.gov/faces/tableservices/jsf/pages/productview.xhtml?pid=PEP_2016_PEPANNRES&prodType=table

- Chan, P. K. S. (2002). Outbreak of Avian Influenza A(H5N1) Virus Infection in Hong Kong in 1997. *Clinical Infectious Diseases*, 34(Supplement_2), S58–S64.
<https://doi.org/10.1086/338820>
- Daugherty, E. L., Carlson, A. L., & Perl, T. M. (2010). Planning for the Inevitable: Preparing for Epidemic and Pandemic Respiratory Illness in the Shadow of H1N1 Influenza. *Clinical Infectious Diseases*, 50(8), 1145–1154. <https://doi.org/10.1086/651272>
- Davis, D. P., Poste, J. C., Hicks, T., Polk, D., Rymer, T. E., & Jacoby, I. (2005). Hospital Bed Surge Capacity in the Event of a Mass-Casualty Incident. *Prehospital and Disaster Medicine*, 20(3), 169–176. <https://doi.org/10.1017/S1049023X00002405>
- Delamater, P. L. (2013). Spatial accessibility in suboptimally configured health care systems: A modified two-step floating catchment area (M2SFCA) metric. *Health & Place*, 24(Supplement C), 30–43. <https://doi.org/10.1016/j.healthplace.2013.07.012>
- Disease Burden of Influenza | Seasonal Influenza (Flu) | CDC. (2017, July 19). Retrieved November 14, 2017, from <https://www.cdc.gov/flu/about/disease/burden.htm>
- Eastman, A. L., Rinnert, K. J., Nemeth, I. R., Fowler, R. L., & Minei, J. P. (2007). Alternate Site Surge Capacity in Times of Public Health Disaster Maintains Trauma Center and Emergency Department Integrity: Hurricane Katrina: *The Journal of Trauma: Injury, Infection, and Critical Care*, 63(2), 253–257.
<https://doi.org/10.1097/TA.0b013e3180d0a70e>
- FluSurge 2.0 | Pandemic Influenza (Flu) | CDC. (n.d.). Retrieved October 4, 2017, from <https://www.cdc.gov/flu/pandemic-resources/tools/flusurge.htm>

- Frost, W. H. (1919). THE EPIDEMIOLOGY OF INFLUENZA. *Journal of the American Medical Association*, 73(5), 313–318.
<https://doi.org/10.1001/jama.1919.02610310007003>
- Frost, W. H. (1920). Statistics of Influenza Morbidity: With Special Reference to Certain Factors in Case Incidence and Case Fatality. *Public Health Reports (1896-1970)*, 35(11), 584–597. <https://doi.org/10.2307/4575511>
- Frost, W. H., & Sydenstricker, E. (1919). Influenza in Maryland: Preliminary Statistics of Certain Localities. *Public Health Reports (1896-1970)*, 34(11), 491–504.
<https://doi.org/10.2307/4575056>
- Gelberg, L., Andersen, R. M., & Leake, B. D. (2000). The Behavioral Model for Vulnerable Populations: application to medical care use and outcomes for homeless people. *Health Services Research*, 34(6), 1273–1302.
- Germann, T. C., Kadau, K., Longini, I. M., & Macken, C. A. (2006). Mitigation strategies for pandemic influenza in the United States. *Proceedings of the National Academy of Sciences*, 103(15), 5935–5940. <https://doi.org/10.1073/pnas.0601266103>
- Guagliardo, M. F. (2004). Spatial accessibility of primary care: concepts, methods and challenges. *International Journal of Health Geographics*, 3, 3.
<https://doi.org/10.1186/1476-072X-3-3>
- H5 Viruses in the United States | Avian Influenza (Flu). (n.d.). Retrieved November 6, 2017, from <https://www.cdc.gov/flu/avianflu/h5/index.htm>
- Hansen, W. G. (1959). How Accessibility Shapes Land Use. *Journal of the American Institute of Planners*, 25(2), 73–76. <https://doi.org/10.1080/01944365908978307>

- Hick, J. L., Barbera, J. A., & Kelen, G. D. (2009). Refining Surge Capacity: Conventional, Contingency, and Crisis Capacity. *Disaster Medicine and Public Health Preparedness*, 3(S1), S59–S67. <https://doi.org/10.1097/DMP.0b013e31819f1ae2>
- How Flu Spreads | Seasonal Influenza (Flu) | CDC. (2017, October 5). Retrieved November 14, 2017, from <https://www.cdc.gov/flu/about/disease/spread.htm>
- How Is Pandemic Flu Different from Seasonal Flu? | Pandemic Influenza (Flu) | CDC. (2017, April 7). Retrieved November 5, 2017, from <https://www.cdc.gov/flu/pandemic-resources/basics/about.html>
- Huff, D. L. (1963). A Probabilistic Analysis of Shopping Center Trade Areas. *Land Economics*, 39(1), 81–90. <https://doi.org/10.2307/3144521>
- Huff, D. L. (1964). Defining and Estimating a Trading Area. *Journal of Marketing*, 28(3), 34–38. <https://doi.org/10.2307/1249154>
- Influenza (Flu) Viruses | Seasonal Influenza (Flu) | CDC. (2017, October 5). Retrieved November 5, 2017, from <https://www.cdc.gov/flu/about/viruses/index.htm>
- Joseph, A. E., & Bantock, P. R. (1982). Measuring potential physical accessibility to general practitioners in rural areas: A method and case study. *Social Science & Medicine*, 16(1), 85–90. [https://doi.org/10.1016/0277-9536\(82\)90428-2](https://doi.org/10.1016/0277-9536(82)90428-2)
- Joshi, A. J. (2008). *Study on the effect of different arrival patterns on an emergency department's capacity using discrete event simulation* (Thesis). Kansas State University. Retrieved from <http://krex.k-state.edu/dspace/handle/2097/1024>
- Karlamangla, S. (n.d.). Severe flu brings medicine shortages, packed ERs and a rising death toll in California. Retrieved April 2, 2018, from <http://www.latimes.com/local/california/la-me-ln-flu-surge-20180106-htmlstory.html>

- Liu, X., & Stechlinski, P. (2017). The Switched SIR Model. In *Infectious Disease Modeling* (pp. 43–82). Springer, Cham. https://doi.org/10.1007/978-3-319-53208-0_3
- Luo, J. (2014). Integrating the Huff Model and Floating Catchment Area Methods to Analyze Spatial Access to Healthcare Services. *Transactions in GIS*, 18(3), 436–448. <https://doi.org/10.1111/tgis.12096>
- Luo, W., & Wang, F. (2003). Measures of Spatial Accessibility to Health Care in a GIS Environment: Synthesis and a Case Study in the Chicago Region. *Environment and Planning B: Planning and Design*, 30(6), 865–884. <https://doi.org/10.1068/b29120>
- Steven Manson, Jonathan Schroeder, David Van Riper, and Steven Ruggles. IPUMS National Historical Geographic Information System: Version 12.0 [Database]. Minneapolis: University of Minnesota. 2017. <http://doi.org/10.18128/D050.V12.0>
- Medina, R. A., Manicassamy, B., Stertz, S., Seibert, C. W., Hai, R., Belshe, R. B., ... García-Sastre, A. (2010). Pandemic 2009 H1N1 vaccine protects against 1918 Spanish influenza virus. *Nature Communications*, 1(3), 1–6. <https://doi.org/10.1038/ncomms1026>
- Menon, D. K., Taylor, B. L., Ridley, S. A., & on behalf of the Intensive Care Society, U. (2005). Modelling the impact of an influenza pandemic on critical care services in England. *Anaesthesia*, 60(10), 952–954. <https://doi.org/10.1111/j.1365-2044.2005.04372.x>
- Monto, A. S., Comanor, L., Shay, D. K., & Thompson, W. W. (2006). Epidemiology of Pandemic Influenza: Use of Surveillance and Modeling for Pandemic Preparedness. *The Journal of Infectious Diseases*, 194(Supplement_2), S92–S97. <https://doi.org/10.1086/507559>

- Morens, D. M., & Fauci, A. S. (2007). The 1918 Influenza Pandemic: Insights for the 21st Century. *The Journal of Infectious Diseases*, 195(7), 1018–1028.
<https://doi.org/10.1086/511989>
- Morrill, R. L., Earickson, R. J., & Rees, P. (1970). Factors Influencing Distances Traveled to Hospitals. *Economic Geography*, 46(2), 161–171. <https://doi.org/10.2307/142624>
- National Pandemic Strategy | Pandemic Influenza (Flu) | CDC. (2017, June 22). Retrieved September 6, 2017, from <https://www.cdc.gov/flu/pandemic-resources/national-strategy/index.html>
- Osterholm, M. T. (2005). Preparing for the Next Pandemic. *New England Journal of Medicine*, 352(18), 1839–1842. <https://doi.org/10.1056/NEJMp058068>
- Pandemic Influenza | Pandemic Influenza (Flu) | CDC. (2017, July 18). Retrieved October 4, 2017, from <https://www.cdc.gov/flu/pandemic-resources/index.htm>
- Past Pandemics | Pandemic Influenza (Flu) | CDC. (2017, November 2). Retrieved November 14, 2017, from <https://www.cdc.gov/flu/pandemic-resources/basics/past-pandemics.html>
- Pérez-Trallero, E., Piñero, L., Vicente, D., Montes, M., & Cilla, G. (2009). Residual immunity in older people against the influenza A(H1N1) – recent experience in northern Spain. *Eurosurveillance*, 14(39), 19344. <https://doi.org/10.2807/ese.14.39.19344-en>
- Schultz, C. H., & Stratton, S. J. (2007). Improving Hospital Surge Capacity: A New Concept for Emergency Credentialing of Volunteers. *Annals of Emergency Medicine*, 49(5), 602–609. <https://doi.org/10.1016/j.annemergmed.2006.10.003>
- Schultz, & Koenig. (2006). State of Research in High-consequence Hospital Surge Capacity - Schultz - 2006 - Academic Emergency Medicine - Wiley Online Library. Retrieved

November 7, 2017, from
<http://onlinelibrary.wiley.com/doi/10.1197/j.aem.2006.06.033/full>

Seasonal Influenza, More Information | Seasonal Influenza (Flu) | CDC. (2017, October 13).
Retrieved November 14, 2017, from <https://www.cdc.gov/flu/about/qa/disease.htm>

Situation Update: Summary of Weekly FluView Report | Seasonal Influenza (Flu) | CDC. (2018, February 9). Retrieved February 10, 2018, from
<https://www.cdc.gov/flu/weekly/summary.htm>

Treatment | Seasonal Influenza (Flu) | CDC. (n.d.). Retrieved February 10, 2018, from
<https://www.cdc.gov/flu/consumer/treatment.htm>

Tumpey, T. M., Basler, C. F., Aguilar, P. V., Zeng, H., Solórzano, A., Swayne, D. E., ... García-Sastre, A. (2005). Characterization of the Reconstructed 1918 Spanish Influenza Pandemic Virus. *Science*, *310*(5745), 77–80. <https://doi.org/10.1126/science.1119392>

Types of Influenza Viruses | Seasonal Influenza (Flu) | CDC. (2017, September 27). Retrieved November 5, 2017, from <https://www.cdc.gov/flu/about/viruses/types.htm>

U.S. Homeland Security Council. (n.d.). National Strategy for Pandemic Influenza.

Uscher-Pines, L., Omer, S. B., Barnett, D. J., Burke, T. A., & Balicer, R. D. (2006). Priority Setting for Pandemic Influenza: An Analysis of National Preparedness Plans. *PLOS Medicine*, *3*(10), e436. <https://doi.org/10.1371/journal.pmed.0030436>

Watson, S. K., Rudge, J. W., & Coker, R. (2013). Health Systems' "Surge Capacity": State of the Art and Priorities for Future Research. *Milbank Quarterly*, *91*(1), 78–122.
<https://doi.org/10.1111/milq.12003>